Supporting Information

Effect of Substitution Position of Dibenzofuran-terminated Robust Hole-transporters on Physical Properties and TADF OLED Performances

Shoki Abe[1], Hisahiro Sasabe[1,2,3], Takeru Nakamura[1], Misaki Matsuya[1], Yu Saito[1], Takanori Hanayama[1], Suguru Araki[1], Kengo Kumada[1], and Junji Kido*[1,2,3]*

[1]Department of Organic Materials Science, Yamagata University, 4-3-16 Jonan, Yonezawa, Yamagata 992-8510, Japan,
[2]Research Center of Organic Electronics (ROEL), Yamagata University, 4-3-16 Jonan, Yonezawa, Yamagata 992-8510, Japan,
[3]Frontier Center for Organic Materials (FROM), Yamagata University, 4-3-16 Jonan, Yonezawa, Yamagata 992-8510, Japan,

E-mail: h-sasabe@yz.yamagata-u.ac.jp

General considerations:

Quantum chemical calculations were performed using the hybrid density functional theory (DFT), functional Becke and Hartree-Fock exchange, and Lee Yang and Parr correlation (B3LYP) as implemented in the Gaussian 09 program packages.[1] Electrons were described by the Pople 6-31G(d,p) and 6-311+G(d,p) basis sets for molecular structure optimization and single-point energy calculations, respectively. The BDEs of the anion, and the neutral states were calculated at the URB3LYP 6-31G(d) level of theory according to the enthalpy change in the corresponding reaction of homolytic cleavage of a single bond in the gas phase at 298 K and 1 atm.[2] The reorganization energy and ionization potential was calculated according to the literature method at the URB3LYP 6-31G(d) level of theory.[3] ^{1}H-NMR and ^{13}C-NMR spectra were recorded on JEOL 400, 500, 600 spectrometers. Mass spectra were obtained using a JEOL JMS-K9 mass spectrometer and a Waters SQD2 mass spectrometer with atmospheric pressure solid analysis probe (ASAP). FT-IR spectra were recorded using Shimadzu IRAffinity-1S spectrophotometer. Differential scanning calorimetry (DSC) was performed using a Perkin-Elmer Diamond DSC Pyris instrument under nitrogen atmosphere at a heating rate of 10 °C min^{-1}. Thermogravimetric analysis (TGA) was undertaken using a SEIKO EXSTAR 6000 TG/DTA 6200 unit under nitrogen atmosphere at a heating rate of 10 °C min^{-1}. UV-Vis spectra were measured using a Shimadzu UV-3150 UV-vis-NIR spectrophotometer. Photoluminescence spectra were measured using a FluroMax-2 (Jobin-Yvon-Spex) luminescence spectrometer. The ionization potential (I_p) was determined using a photoelectron yield spectroscopy (PYS) in vacuum (~10^{-3} Pa).[4] The phosphorescent spectra were measured using a streak camera (C4334 from Hamamatsu Photonics) at 5K.

Device Fabrication and Characterization:

NPD and **Liq** were purchased from e-Ray Optoelectronics Technology Co., Ltd. **DBF-TRZ**[5] and **nBPhen** were purchased from Flask. **mCBP**[6], **4CzIPN**[7], were prepared according to the previous reports. The UPLC purities for HTLs were 99.7% for **T1DBFBP** (H_2O/THF/HCOOH = 7/12/1 (vol)), 99.6% for **T2DBFBP** (H_2O/THF/HCOOH = 7/12/1 (vol)), 100% for **T3DBFBP** H_2O/THF/HCOOH = 7/12/1 (vol)). All organic materials were purified by temperature gradient sublimation in vacuum. The substrates were cleaned with ultra-purified water and organic solvents (acetone and then isopropanol), and then dry-cleaned for 30 min by exposure to UV-ozone. The organic layers were deposited onto the ITO substrate in vacuum (ca. 10^{-5} Pa) successively. Al was patterned using a shadow mask with an array of 2 mm × 2 mm openings without breaking the vacuum (ca. 10^{-5} Pa). The EL spectra were taken using an optical

multichannel analyzer Hamamatsu Photonics PMA-11. The current density–voltage and luminance–voltage characteristics were measured using a Keithley source measure unit 2400 and a Minolta CS200 luminance meter, respectively.

References:

[1] *Gaussian 09*, Revision D.01, M. J. Frisch, G. W. Trucks, H. B. Schlegel, G. E. Scuseria, M. A. Robb, J. R. Cheeseman, G. Scalmani, V. Barone, B. Mennucci, G. A. Petersson, H. Nakatsuji, M. Caricato, X. Li, H. P. Hratchian, A. F. Izmaylov, J. Bloino, G. Zheng, J. L. Sonnenberg, M. Hada, M. Ehara, K. Toyota, R. Fukuda, J. Hasegawa, M. Ishida, T. Nakajima, Y. Honda, O. Kitao, H. Nakai, T. Vreven, J. A. Montgomery, Jr., J. E. Peralta, F. Ogliaro, M. Bearpark, J. J. Heyd, E. Brothers, K. N. Kudin, V. N. Staroverov, R. Kobayashi, J. Normand, K. Raghavachari, A. Rendell, J. C. Burant, S. S. Iyengar, J. Tomasi, M. Cossi, N. Rega, J. M. Millam, M. Klene, J. E. Knox, J. B. Cross, V. Bakken, C. Adamo, J. Jaramillo, R. Gomperts, R. E. Stratmann, O. Yazyev, A. J. Austin, R. Cammi, C. Pomelli, J. W. Ochterski, R. L. Martin, K. Morokuma, V. G. Zakrzewski, G. A. Voth, P. Salvador, J. J. Dannenberg, S. Dapprich, A. D. Daniels, Ö. Farkas, J. B. Foresman, J. V. Ortiz, J. Cioslowski, and D. J. Fox, Gaussian, Inc., Wallingford CT, **2013**.

[2] (a) N. Lin, J. Qiao, L. Duan, L. Wang, Y. Qiu, *J. Phys. Chem. C.* **2014**, *118*, 7569; (b) M. Hong, M. K. Ravva, R. Winget, J.-L. Bredas, *Chem. Mater.* **2016**, *28*, 5791.

[3] (a) V. Coropceanu, O. Kwon, B. Wex, B. R. Kaafarani, N. E. Gruhn, J. C. Durivage, D. C. Neckers, J.-L. Brédas, *Chem. Eur. J.* **2006**, *12*, 2073; (b) E. Varathan, D. Vijay, V. Subramanian, *J. Phys. Chem. C* **2014**, *118*, 21741.

[4] H. Ishii, D. Tsunami, T. Suenaga, N. Sato, Y. Kimura, M. Niwano, *J. Surf. Sci. Soc. Jpn.* **2007**, *28*, 264.

[5] a) Y. Nagai, H. Sasabe, J. Takahashi, N. Onuma, T. Ito, S. Ohisa, J. Kido, *J. Mater. Chem. C* **2017**, *5*, 527; b) T. Ito, H. Sasabe, Y. Nagai, Y. Watanabe, N. Onuma, J. Kido, *Chem. Eur. J.* **2019**, *25*, 7308.

[6] P. Schrögel, N. Langer, C. Shildknecht, G. Wagenblast, C. Lennartz, P. Strohriegl, *Org. Electron.* **2011**, *12*, 2047.

[7] H. Uoyama, K. Goushi, K. Shizu, H. Nomura, C. Adachi, *Nature* **2012**, *492*, 234.

[8] a) E. C. Riesgo, X. Jin, R. P. Thummel, *J. Org. Chem.* **1996**, *61*, 3017; b) Y.-J. Pu, G. Nakata, H. Satoh, H. Sasabe, D. Yokoyama, J. Kido, *Adv. Mater.* **2012**, *24*, 1765.

[9] Y.-J. Pu, M. Miyamoto, K.-I. Nakayama, T. Oyama, Y. Masaaki, J. Kido, *Org. Electron.* **2009**, *10*, 228.

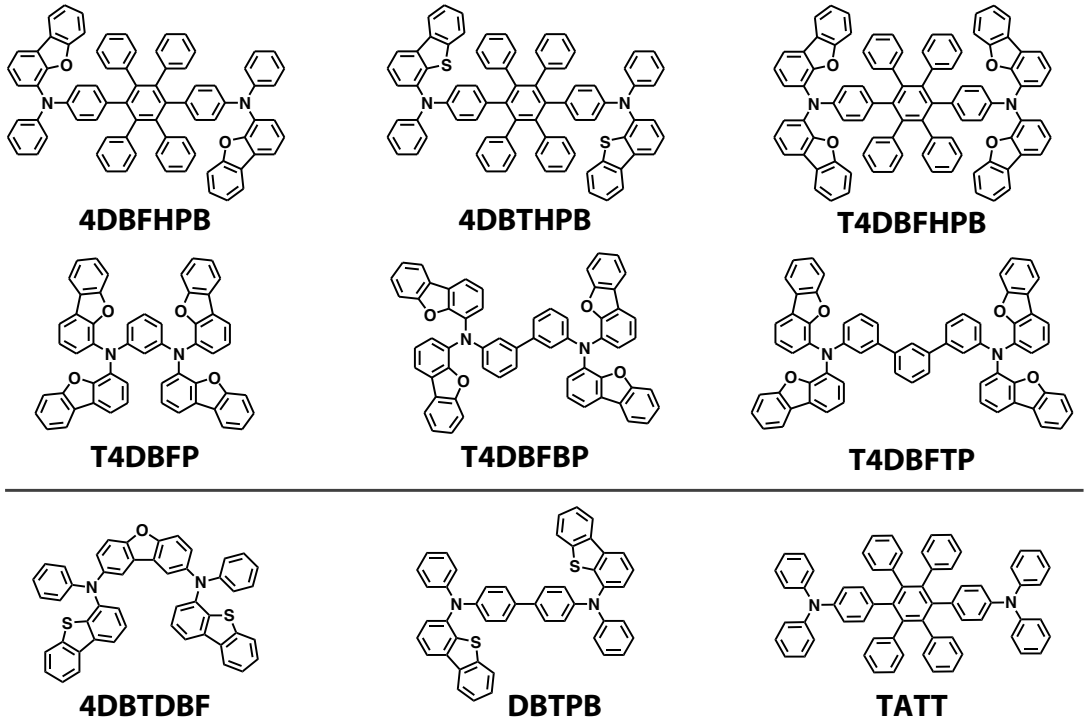

Table S1. Summary of **4CzIPN**-based TADF OLEDs using DBF-end-capped HTLs.

HTL	EQE at 1000 cd/m^2(%)	LT_{50} at 1000 cd/m^2 (h)	Anionic BDE (eV)[a]	Mobility (cm^2/Vs)	Ref
T1DBFBP	20.9	30000	1.43	6.9 x 10^{-5}	This work
T2DBFBP	17.1	25000	1.75	1.8 x 10^{-3}	This work
T3DBFBP	16.4	24000	1.63	2.6 x 10^{-3}	This work
T4DBFBP	21.0	27000	1.61	3.9 x 10^{-4}	This work
4DBFHPB	21.1	20000	1.80	1.5 x 10^{-3}	[10]
4DBTHPB	19.2	24000	1.77	1.5 x 10^{-3}	[10]
T4DBFHPB	22.0	28000	1.72	6.0 x 10^{-4}	[11]
T4DBFP	21.0	27000	1.56	2.5 x 10^{-6}	[12]
T4DBFBP	19.4	20645	1.61	3.9 x 10^{-4}	[12]
T4DBFTP	22.4	22413	1.60	1.7 x 10^{-7}	[12]
4DBTDBF	18.1	6000	-	-	[13]
DBTPB	9.7	5000	-	-	[13]
TATT	20.8	12000	1.52	5.6 x 10^{-6}	[10]

[a]Calculated at TD-DFT RB3LYP/ 6-31G(d)// RB3LYP/ 6-31G(d) level. [b]Calculated at UB3LYP/ 6-31G(d)// UB3LYP/ 6-31G(d) level.

[10] T. Kamata, H. Sasabe, N. Ito, Y. Sukegawa, A. Arai, T. Chiba, D. Yokoyama, J. Kido, *J. Mater. Chem. C* **2020**, *8*, 7200.

[11] N. Nagamura, H. Sasabe, H. Sato, T. Kamata, N. Ito, S. Araki, S. Abe, Y. Sukegawa, D. Yokoyama, H. Kaji, J. Kido, *J. Mater. Chem. C* **2022**, *10*, 8694.

[12] H. Sasabe, S. Araki, S. Abe, N. Ito, K. Kumada, T. Noda, Y. Sukegawa, D. Yokoyama, J. Kido, *Chem. Eur. J.* **2022**, *13*, e202104408.

[13] T. Kamata, H. Sasabe, M. Igarashi, J. Kido, *Chem. Eur. J.* **2018**, *24*, 4590.

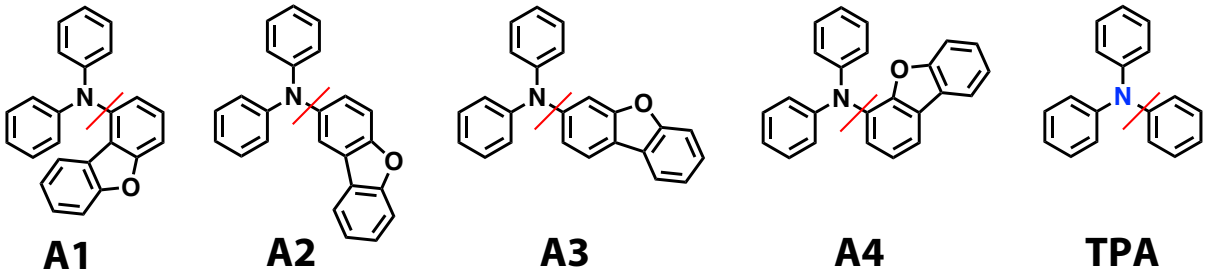

Table S2. Calculated optoelectronic properties

Compound	HOMO/LUMO/E_T (eV) [a]	BDE (eV)[b]
A1	-5.08/–0.97/2.92	1.50
A2	-4.93/–1.00/2.97	1.56
A3	-4.94/–0.94/2.77	1.57
A4	-4.99/–0.95/2.89	1.53
TPA	-4.98/–0.29/3.22	0.87

[a]Calculated at TD-DFT RB3LYP/ 6-31G(d)// RB3LYP/ 6-31G(d) level. [b]Calculated at UB3LYP/ 6-31G(d)// UB3LYP/ 6-31G(d) level.

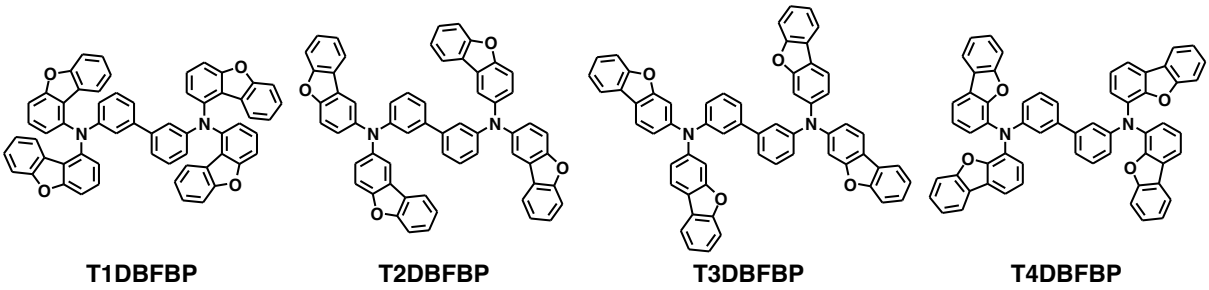

Table S3. Calculated ionization potential (IP) and reorganization energy of cation state (λ).

Compound	IP (eV) [a]	λ (meV)[a]
T1DBFBP	6.06	121
T2DBFBP	5.76	113
T3DBFBP	5.79	68
T4DBFBP	5.90	110

[a]Calculated at UB3LYP/ 6-31G(d)// UB3LYP/ 6-31G(d) level.

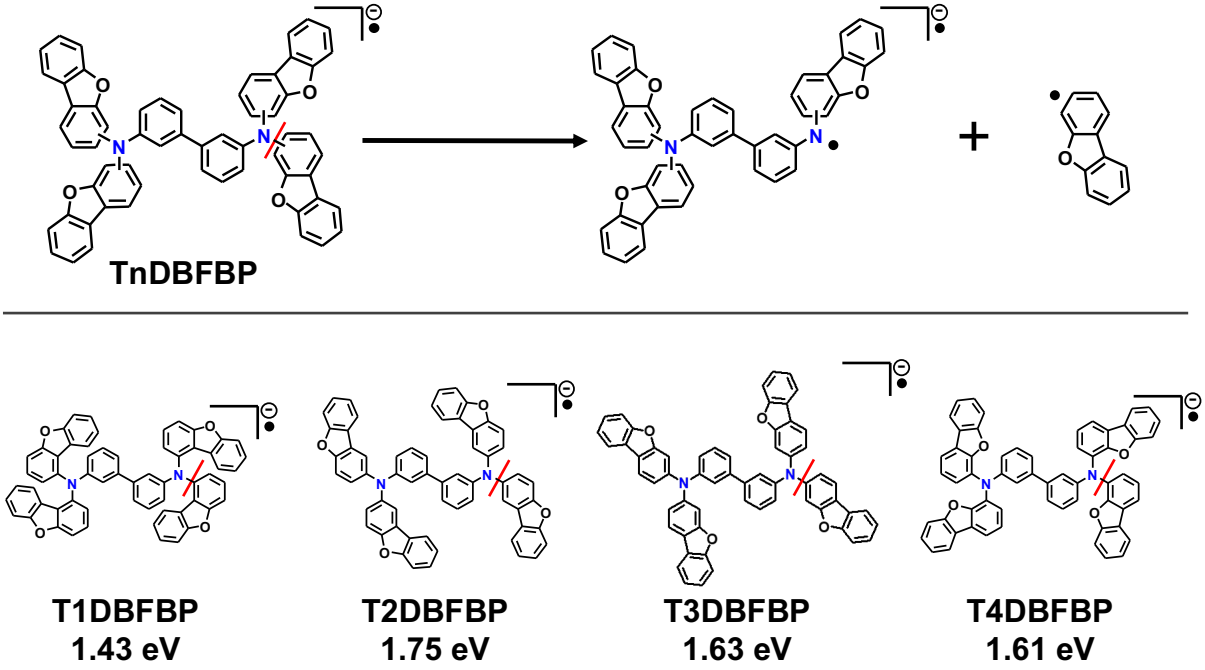

Figure S1. BDEs of **TnDBFBP** derivatives for the anion states calculated at the UB3LYP/ 6-31G(d)// UB3LYP/ 6-31 (d) level of theory.

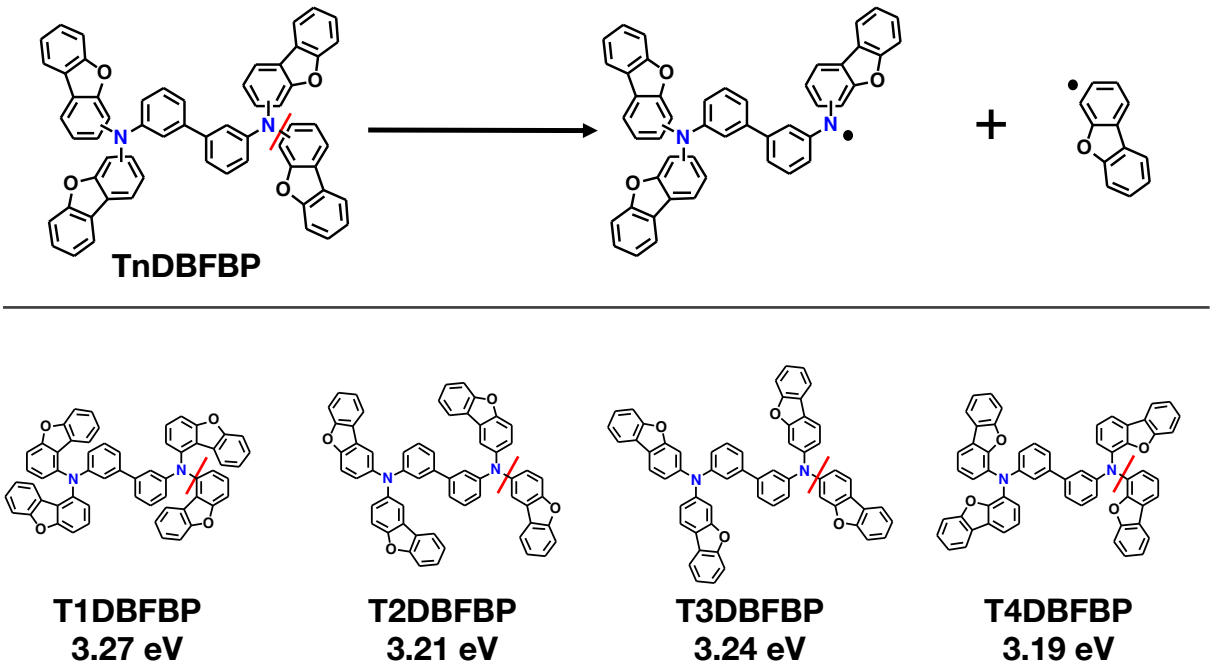

Figure S2. BDEs of **TnDBFBP** derivatives for the neutral states calculated at the UB3LYP/ 6-31G(d)// UB3LYP/ 6-31 (d) level of theory.

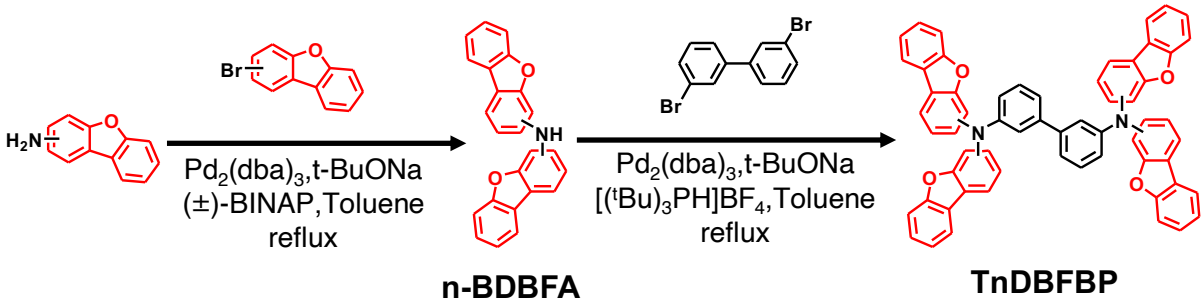

n-BDBFA **TnDBFBP**

Scheme S1. Synthetic route of **TnDBFBP** derivatives.

Synthesis of 1-BDBFA:

Dibenzo[*b,d*]furan-1-amine (2.2 g, 12.0 mmol), 1-bromodibezofuran (3.0 g, 12.1 mmol) and sodium-*t*-butoxide (3.1 g, 32.3 mmol) were added to a round bottom flask. Dry toluene (120 mL) was added to the mixture, and nitrogen (N_2) bubbled through the mixture for 1 h. Then, $Pd_2(dba)_3$ (449 mg, 0.48 mmol) and BINAP (678 mg, 1.09 mmol) were added and the resultant mixture was stirred for 17 h at reflux temperature under the N_2 flow. The mixture was filtered through the silica gel pad and evaporated to dryness, then, washed with methanol to afford **1-BDBFA** (3.4 g, 82%) as a pale yellow solid: ^{1}H-NMR (400 MHz, DMSO-d_6) δ 8.73 (s, 1H), 7.70 (d, J = 8.4 Hz, 2H), 7.63 (d, J = 7.6 Hz, 2H), 7.44 (t, J = 7.6 Hz, 2H), 7.36 (d, J = 4.0 Hz, 4H), 7.21 (t, J = 7.6 Hz, 2H), 6.84 (t, J = 4.4 Hz, 2H) ppm; ^{13}C-NMR (151 MHz, $CDCl_3$) δ 157.4, 155.8, 138.4, 128.4, 127.7, 126.8, 126.2, 123.4, 123.2, 122.4, 121.9, 115.5, 113.1, 112.1, 111.5, 111.4, 106.1, 105.3 ppm; MS: m/z = 350 $[M+H]^+$ (ASAP). IR (powder cm^{-1}) 3378, 3069, 2348, 2329, 2030, 1596, 1582, 1501, 1474, 1447, 1428, 1395, 1300, 1235, 1196, 1110, 1063, 847, 784, 745, 720, 558.

Other **n-BDBFA** derivatives were prepared according to the similar method.

2-BDBFA (1.8 g, 75%) as a pale gray solid: ^{1}H-NMR (400 MHz, DMSO-d_6) δ 8.24 (s, 1H), 8.11 (d, J = 7.2 Hz, 2H), 7.83 (d, J = 2.0 Hz, 2H), 7.66 (d, J = 8.4 Hz, 2H), 7.61 (d, J = 8.4 Hz, 2H), 7.52-7.47 (m, 2H), 7.35 (t, J = 7.2 Hz, 2H), 7.27 (dd, J = 9.2, 2.4 Hz, 2H) ppm; ^{13}C-NMR (151 MHz, $CDCl_3$) δ 172.8, 167.7, 167.7, 156.0, 143.5, 142.8, 141.0, 140.2, 138.8, 138.1, 136.7, 135.6, 135.6, 134.9, 134.8, 128.5, 128.0, 127.9, 127.7, 127.5, 125.8, 125.7 ppm; MS: m/z = 350 $[M+H]^+$ (ASAP). IR (powder cm^{-1}) 3399, 3044, 1596, 1511, 1478, 1447, 1310, 1299, 1277, 1194, 1154, 1115, 1100, 926, 865, 843, 834, 805, 747, 720, 687, 627, 602, 562.

3-BDBFA (1.8 g, 46%) as a pale yellow solid: ^{1}H-NMR (400 MHz, $CDCl_3$) δ 8.94 (s, 1H), 8.01-7.99 (m, 4H), 7.62 (d, J = 8.0 Hz, 2H), 7.45 (d, J = 1.6 Hz, 2H), 7.43-7.39 (m, 2H), 7.37-

7.33 (m, 2H), 7.21 (dd, J = 8.4, 2.0 Hz, 2H) ppm; ^{13}C-NMR (151 MHz, $CDCl_3$) δ 157.8, 156.6, 143.0, 126.4, 125.8, 125.7, 124.7, 123.4, 122.6, 121.6, 120.0, 118.4, 114.8, 113.9, 101.4, 100.4 ppm; MS: m/z = 350 $[M+H]^+$ (ASAP). IR (powder cm^{-1}) 3414, 3056, 1632, 1599, 1515, 1457, 1432, 1356, 1324, 1270, 1189, 1164, 1125, 1017, 971, 934, 845, 818, 799, 762, 747, 722.

Synthesis of **T1DBFBP**:

1,3-Dibromobenzene (0.62 g, 3.0 mmol), **1-BDBFA** (1.7 g, 6.0 mmol), and sodium-t-butoxide (1.0 g, 15.6 mmol) were added to a round bottom flask. Next, dry toluene (60 mL) was added to the mixture, and nitrogen (N_2) bubbled through the mixture for 1 h. Then, $Pd_2(dba)_3$ (117 mg, 0.20 mmol) and tris-t-butylphosphonium tetrafluoroborate (190 mg, 0.40 mmol) were added and the resultant mixture was stirred for 18 h at reflux temperature under the N_2 flow. The mixture was filtered through the silica gel pad and evaporated to dryness. The resulting solid was purified by chromatography on the silica gel (eluent: toluene/hexane = 1/2 v/v). Repetitive recrystallization from ethyl acetate afforded **T1DBFBP** (0.48 g, 29%) as a white solid: ^{1}H-NMR (600 MHz, $CDCl_3$) δ 7.41-7.38 (m, 8H), 7.31-7.26 (m, 5H), 7.25-7.23 (m, 3H), 7.06-7.01 (m, 6H), 6.91-6.79 (m, 10H), 6.74 (d, J = 7.8 Hz, 2H), 6.68 (s, 2H) ppm; ^{13}C-NMR (151 MHz, $CDCl_3$) δ 157.4, 155.9, 155.8, 147.3, 142.2, 141.2, 129.5, 127.8, 127.7, 126.7, 123.2, 122.6, 122.5, 120.8, 120.5, 119.9, 110.9, 110.9, 108.4, 108.3 ppm; MS: m/z 849 $[M+H]^+$. (ASAP) Anal. Calcd for $C_{60}H_{36}N_2O_4$: C, 84.89; H, 4.27; N, 3.30; O, 7.54%. Found: C, 85.04; H, 4.23; N, 3.32%. IR (powder cm^{-1}) 3031, 2195, 2180, 2157, 2043, 1592, 1572, 1540, 1513, 1476, 1449, 1420, 1341, 1310, 1235, 1198, 1110, 1073, 849, 784, 749, 718, 701, 521.

Other **TnDBFBP** derivatives were prepared according to the similar method.

T2DBFBP (1.01 g, 60%) as a white solid: ^{1}H-NMR (600 MHz, $CDCl_3$) δ 7.77 (d, J = 7.8 Hz, 4H), 7.70 (d, J = 1.8 Hz, 4H), 7.55 (d, J = 8.4 Hz, 4H), 7.45-7.42 (m, 4H), 7.41 (d, J = 9.0 Hz, 4H), 7.28-7.27 (m, 5H), 7.26-7.25 (m, 3H), 7.22-7.20 (m, 4H), 7.06 (d, J = 7.2 Hz, 2H), 6.99 (dd, J = 7.8, 1.8 Hz, 2H) ppm; ^{13}C-NMR (151 MHz, $CDCl_3$) δ 156.8, 152.7, 149.4, 143.6, 142.1, 129.5, 127.3, 125.3, 125.3, 124.1, 122.6, 120.8, 120.6, 120.3, 120.1, 117.3, 112.4, 111.7 ppm; m/z 849 $[M+H]^+$. (ASAP) Anal. Calcd for $C_{60}H_{36}N_2O_4$: C, 84.89; H, 4.27; N, 3.30; O, 7.54%. Found: C, 84.97; H, 4.09; N, 3.30%. IR (powder cm^{-1}) 3056, 2153, 2030, 1594, 1570, 1474, 1447, 1412, 1322, 1273, 1229, 1191, 1117, 1042, 1023, 870, 841, 809, 784, 747, 726, 697, 612, 577, 560.

T3DBFBP (1.73 g, 75%) as a white solid: ^{1}H-NMR (600 MHz, $CDCl_3$) δ 7.86 (d, J = 7.2 Hz, 4H), 7.76 (d, J = 7.8 Hz, 4H), 7.49 (d, J = 8.4 Hz, 4H), 7.41-7.38 (m, 6H), 7.33-7.27 (m, 10H),

7.20 (d, J = 7.8 Hz, 2H), 7.15 (dd, J = 8.4, 2.4 Hz, 4H), 7.11 (dd, J = 8.4, 1.2 Hz, 2H) ppm; ^{13}C-NMR (151 MHz, $CDCl_3$) δ 157.2, 156.6, 148.2, 147.5, 129.8, 126.3, 124.2, 123.7, 123.2, 122.8, 122.3, 120.9, 120.1, 119.8, 119.6, 111.5, 107.4 ppm; MS: m/z 849 $[M+H]^+$. (ASAP) Anal. Calcd for $C_{60}H_{36}N_2O_4$: C, 84.89; H, 4.27; N, 3.30; O, 7.54%. Found: C, 85.07; H, 3.72; N, 3.31%. IR (powder cm^{-1}) 3058, 2028, 1632, 1592, 1542, 1495, 1457, 1351, 1312, 1297, 1266, 1235, 1165, 1123, 1042, 1017, 847, 830, 811, 785, 743, 720, 704, 676, 596, 579.

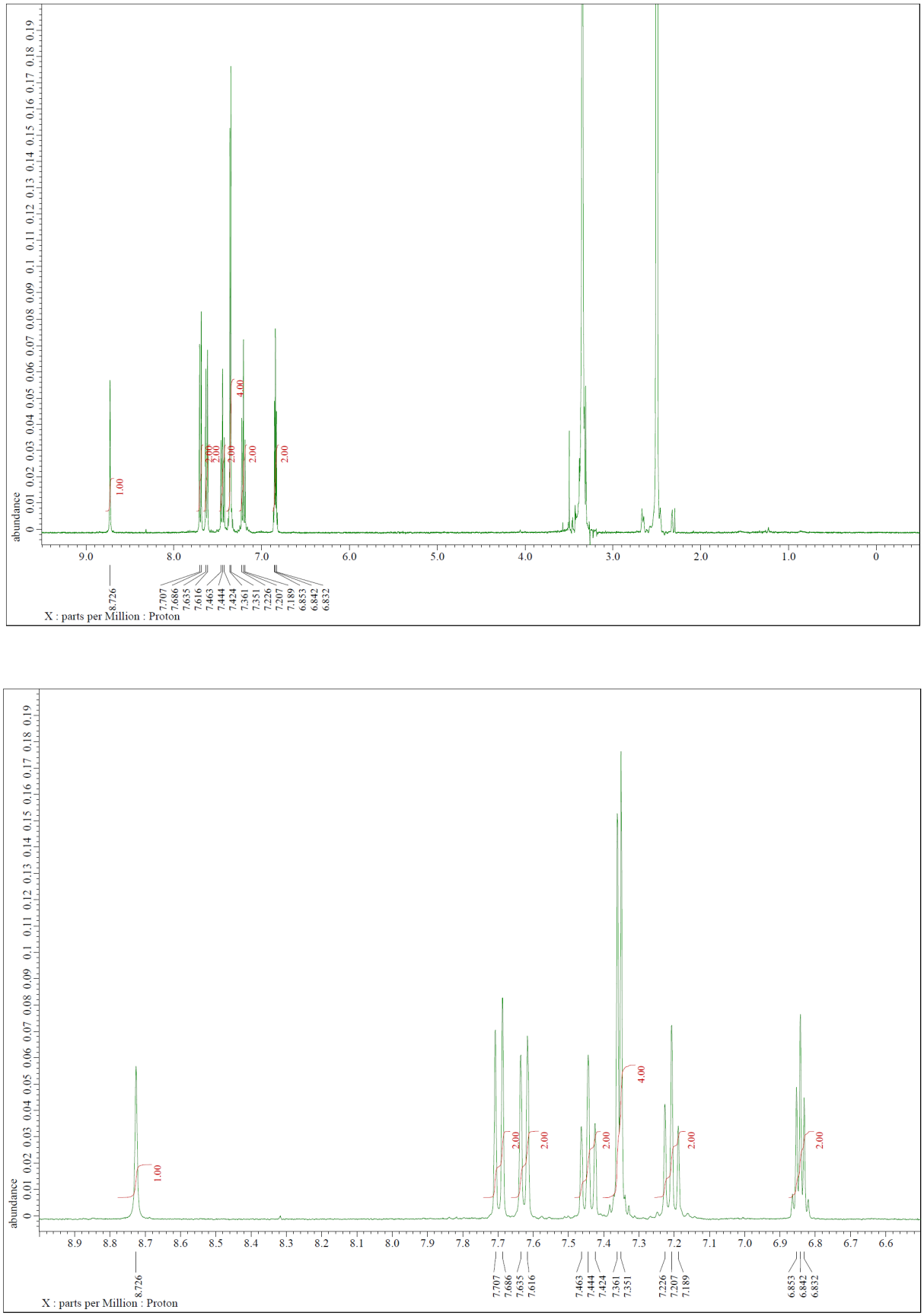

Figure S3. ^{1}H-NMR spectrum of **1-BDBFA** (400 MHz, DMSO-d_6, @R.T.)

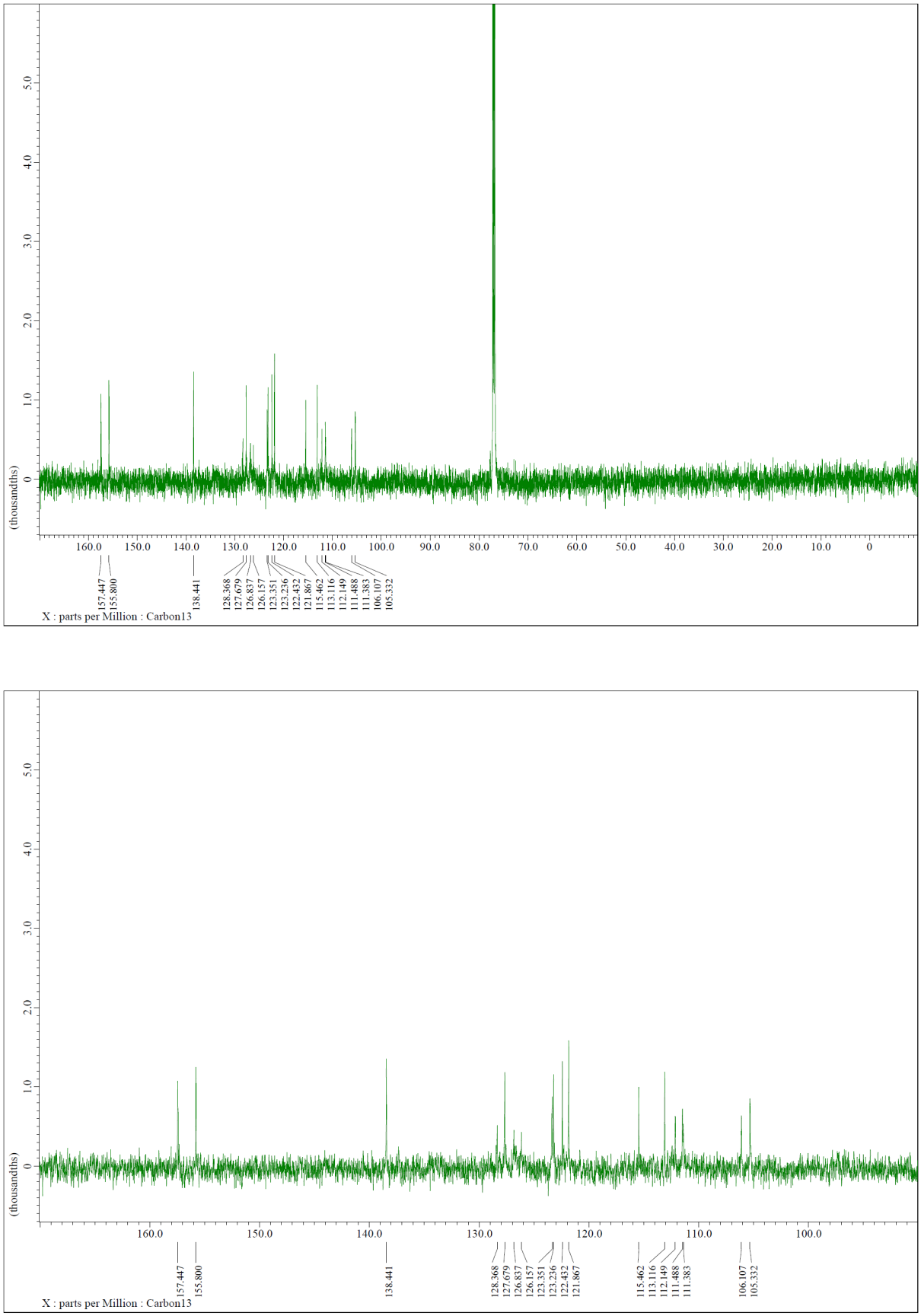

Figure S4. ^{13}C-NMR spectrum of **1-BDBFA** (151 MHz, $CDCl_3$, @R.T.)

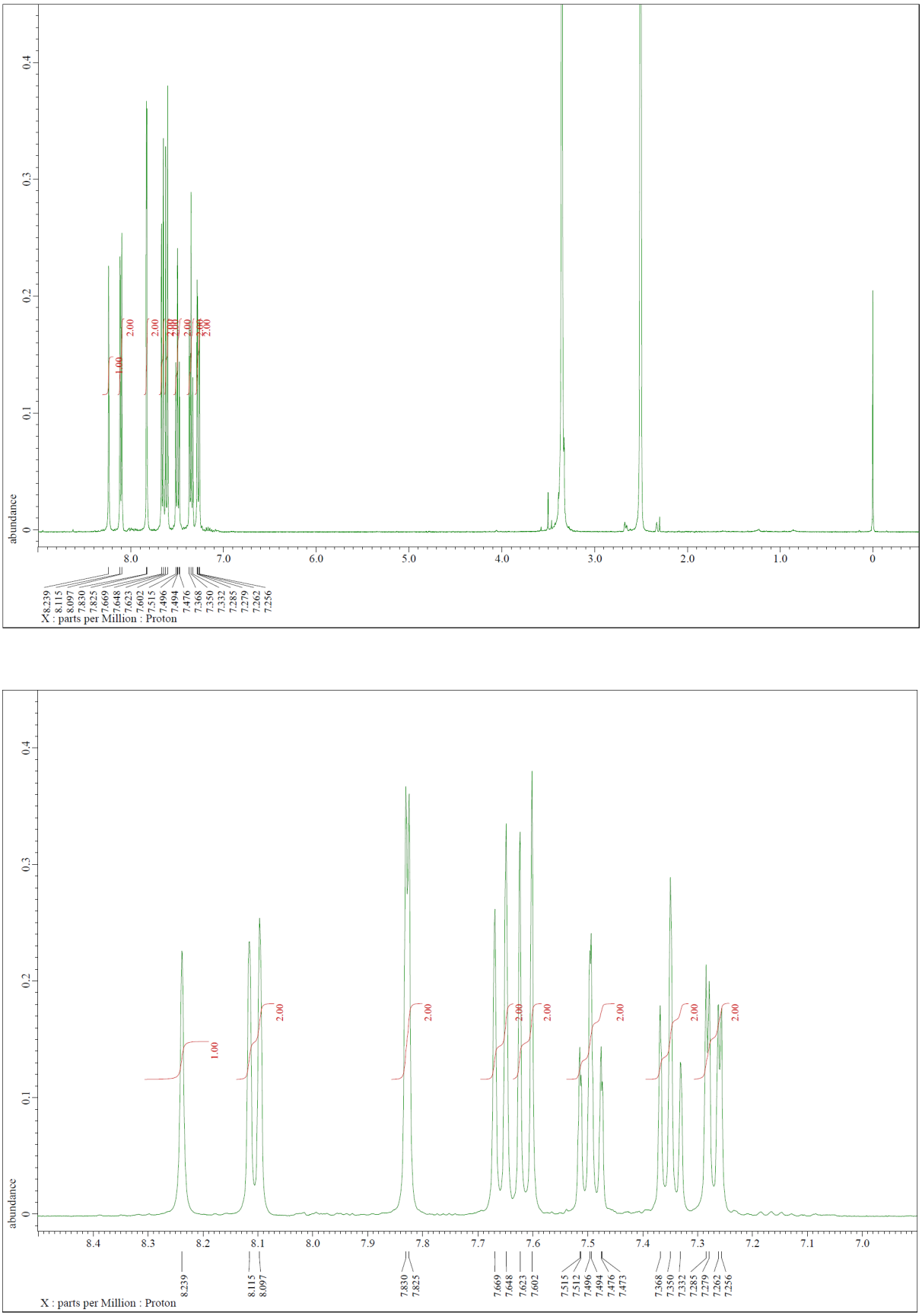

Figure S5. ^{1}H-NMR spectrum of **2-BDBFA** (400 MHz, DMSO-d_6, @R.T.)

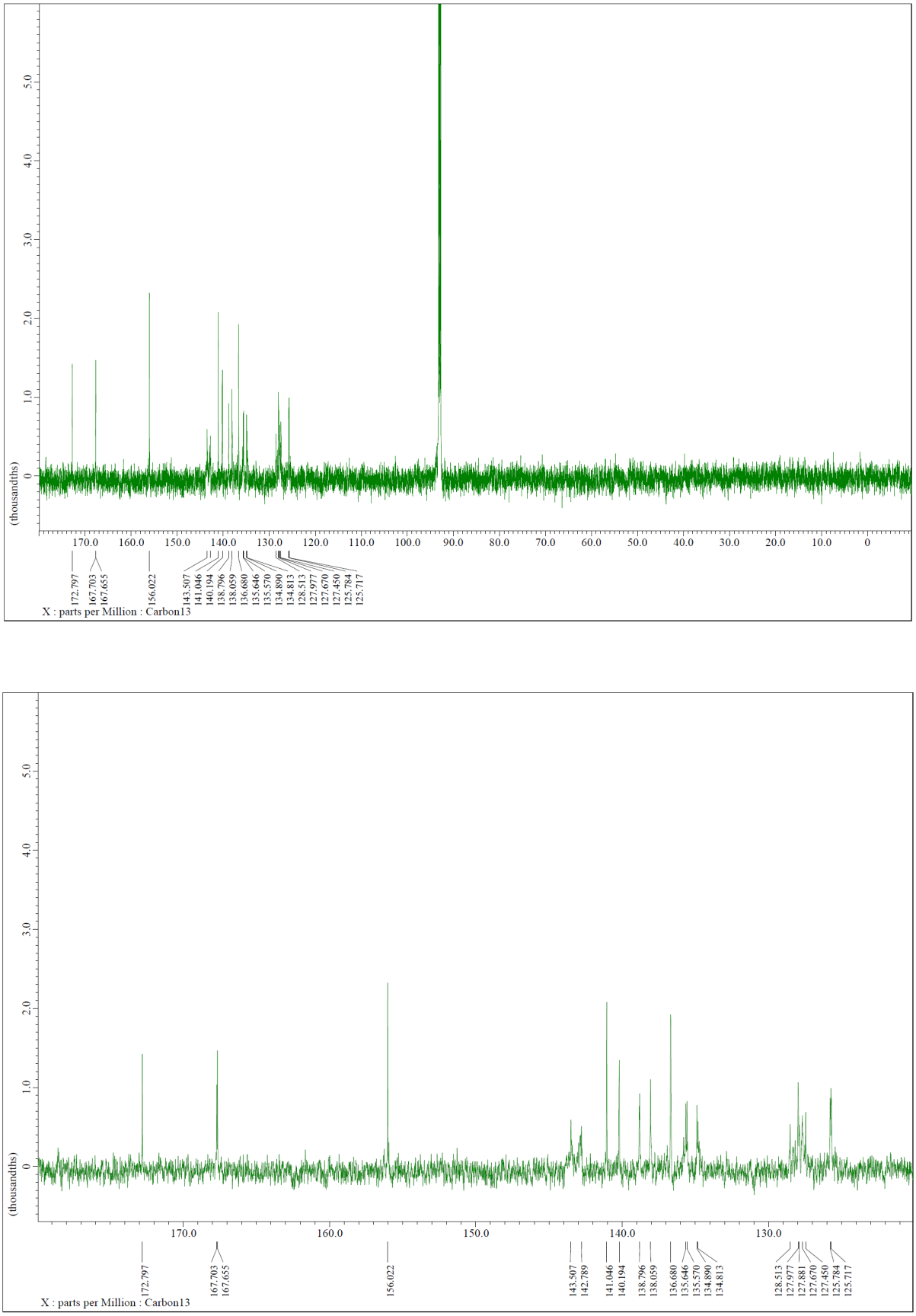

Figure S6. ^{13}C-NMR spectrum of **2-BDBFA** (151 MHz, $CDCl_3$, @R.T.)

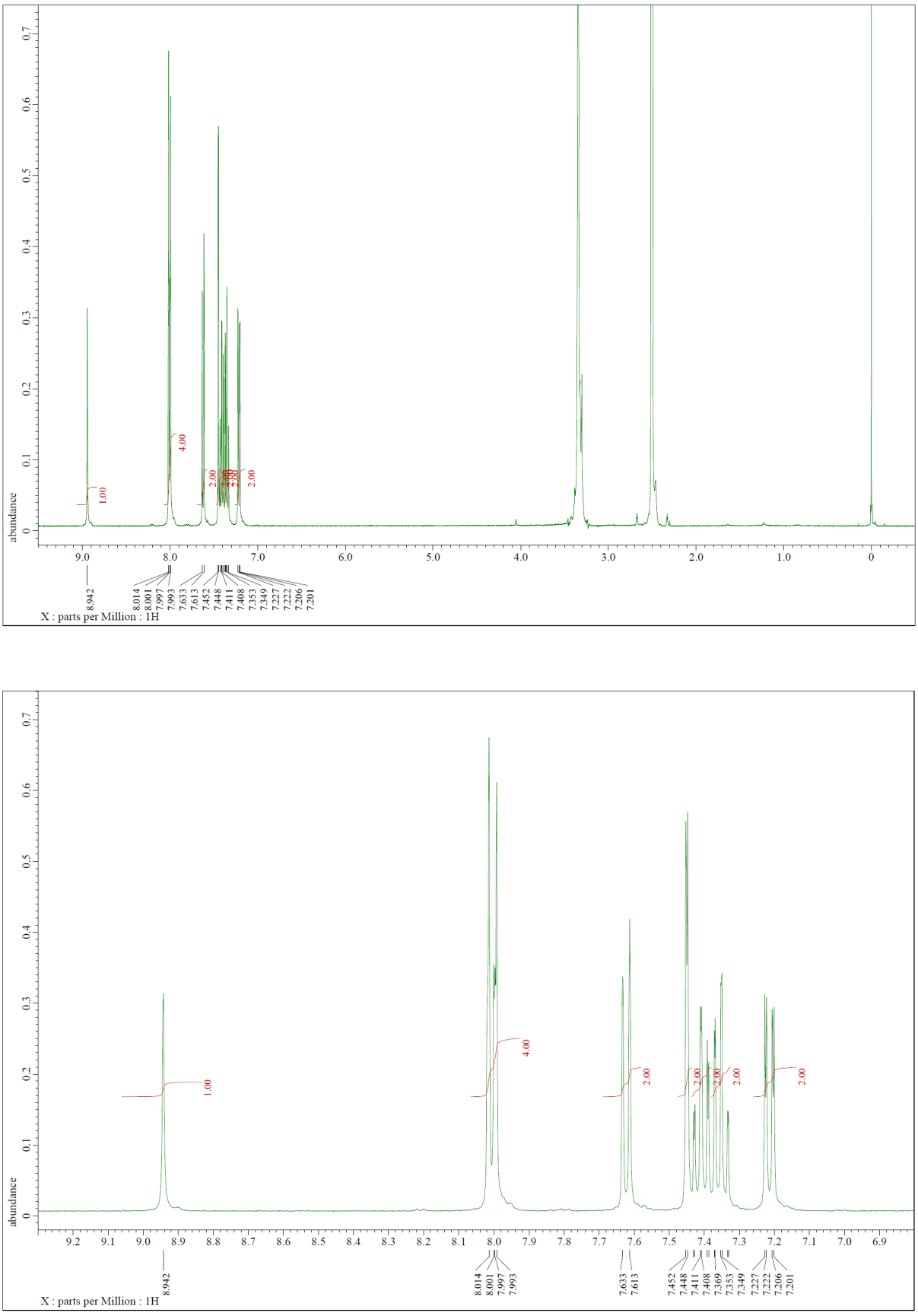

Figure S7. ^{1}H-NMR spectrum of **3-BDBFA** (400 MHz, $CDCl_3$, @R.T.)

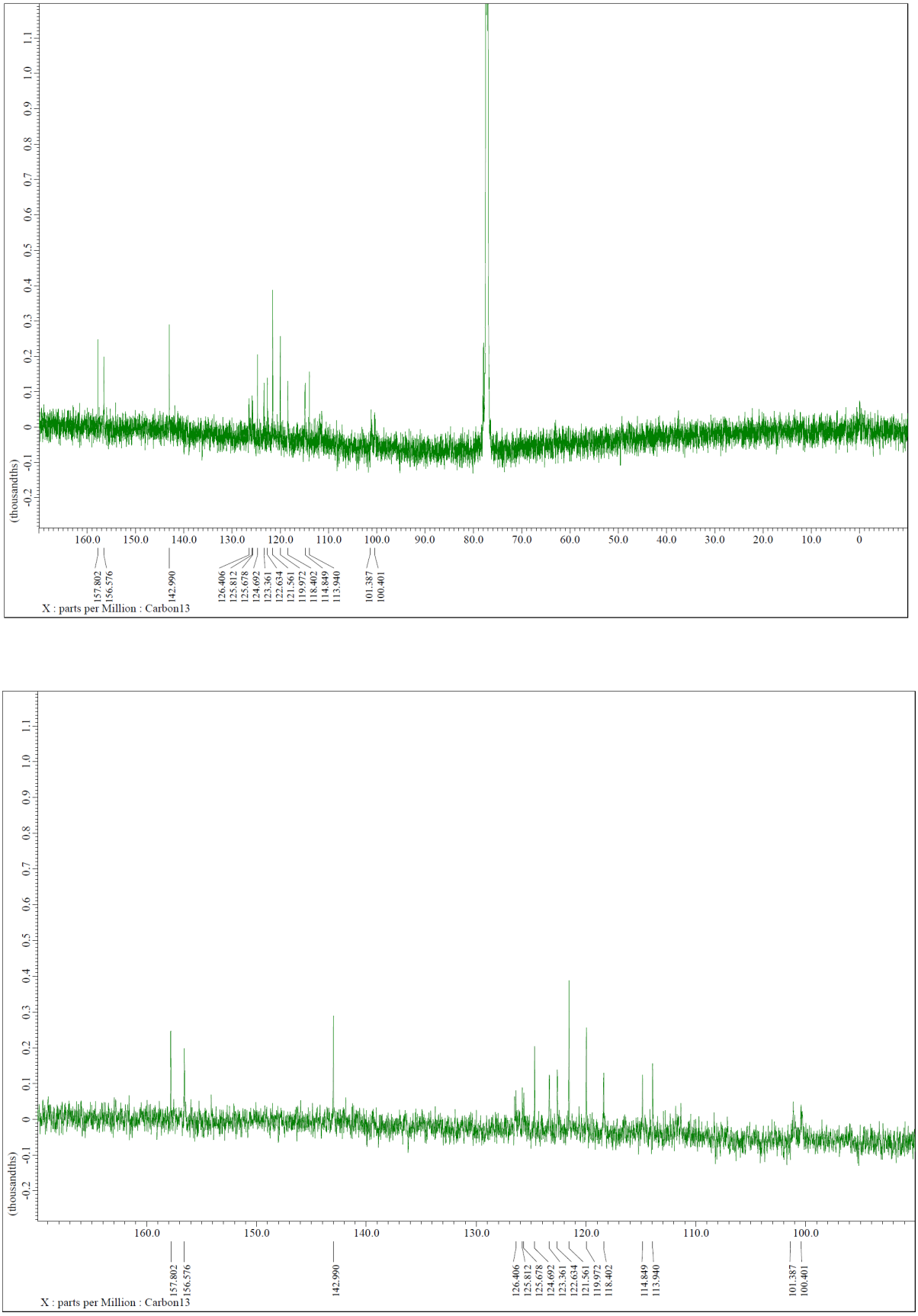

Figure S8. ^{13}C-NMR spectrum of **3-BDBFA** (151 MHz, $CDCl_3$, @R.T.)

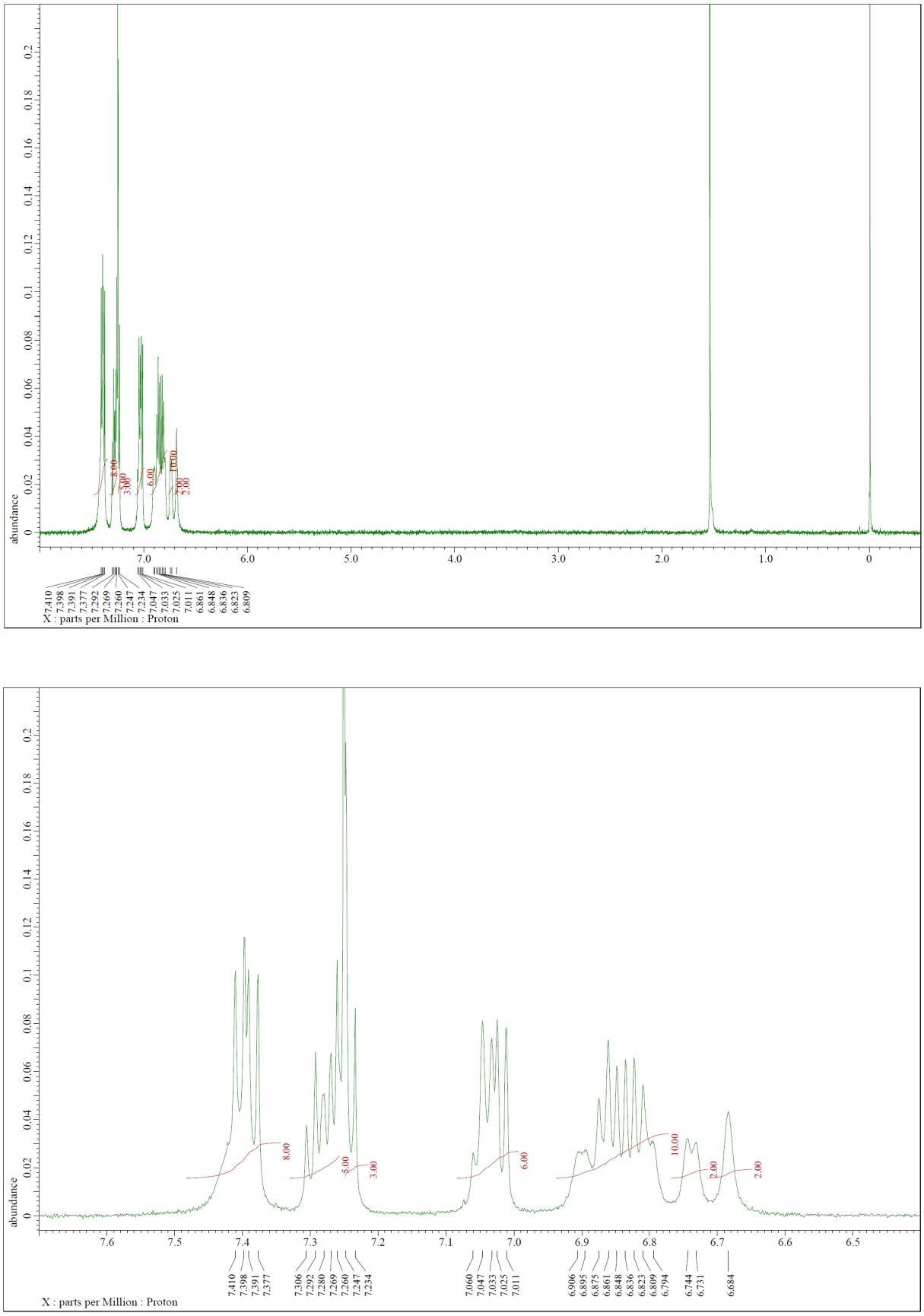

Figure S9. ^{1}H-NMR spectrum of **T1DBFBP** (600 MHz, $CDCl_3$, @R.T.)

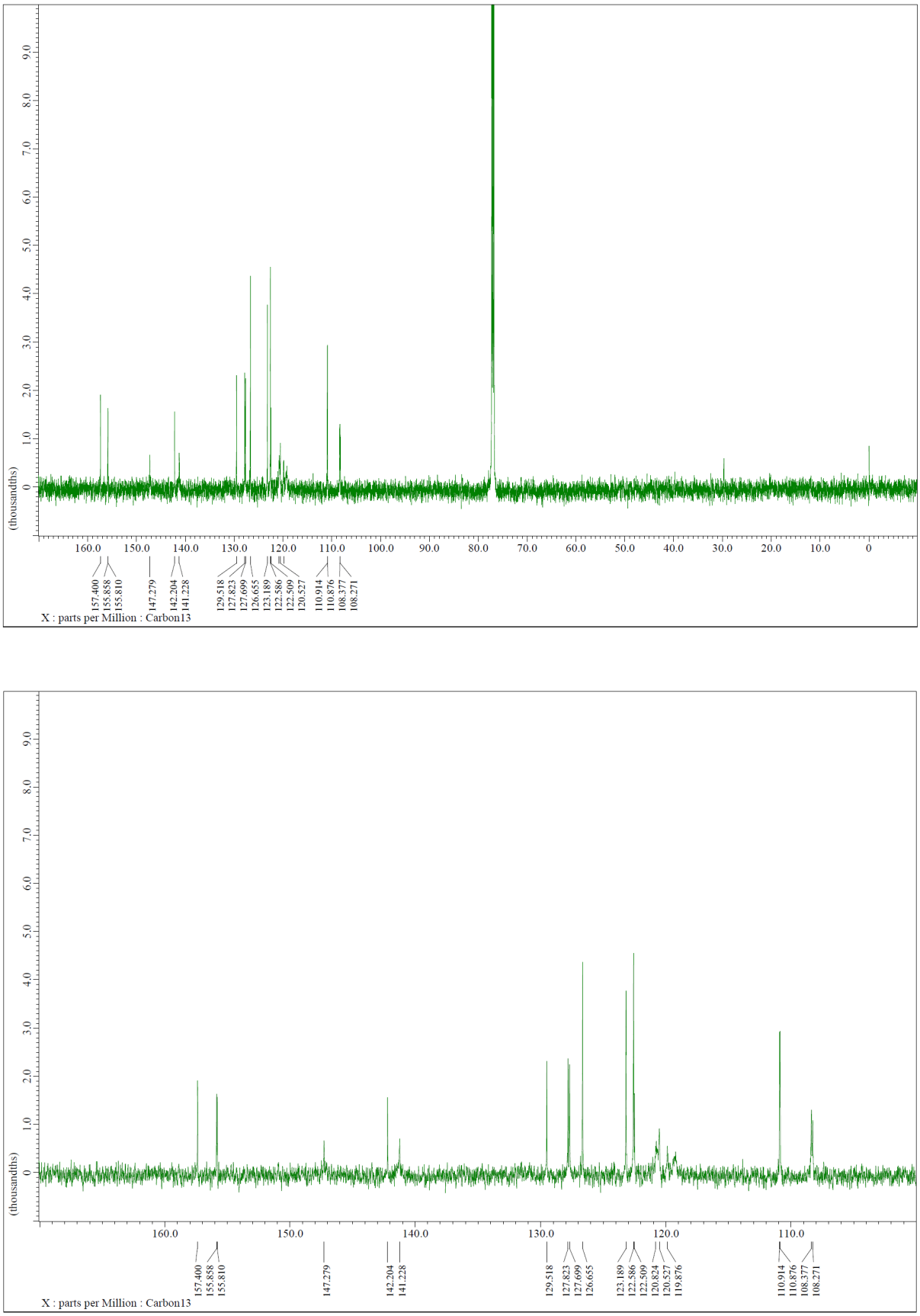

Figure S10. ^{13}C-NMR spectrum of **T1DBFBP** (151 MHz, $CDCl_3$, @R.T.)

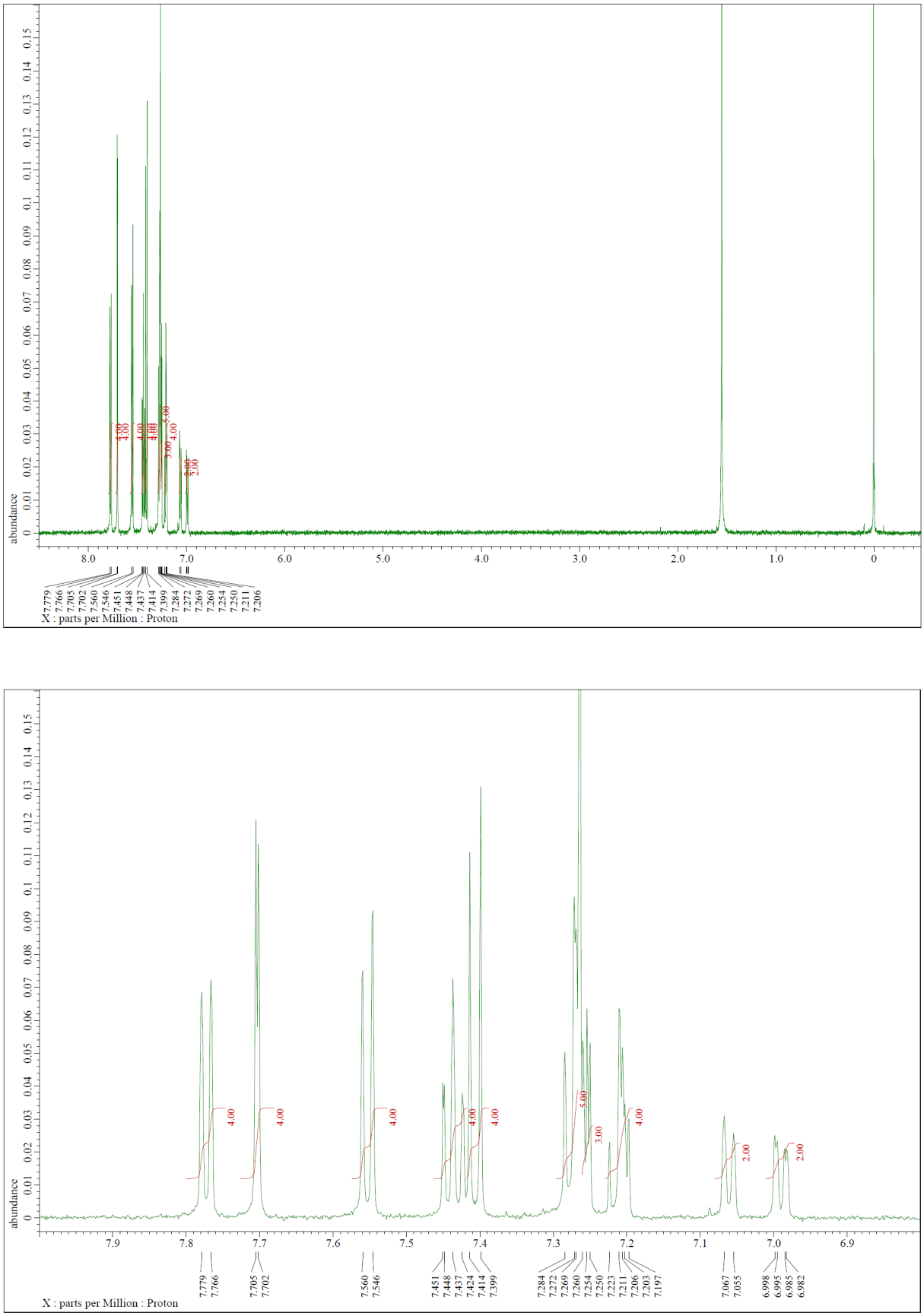

Figure S11. ^{1}H-NMR spectrum of **T2DBFBP** (600 MHz, $CDCl_3$, @R.T.)

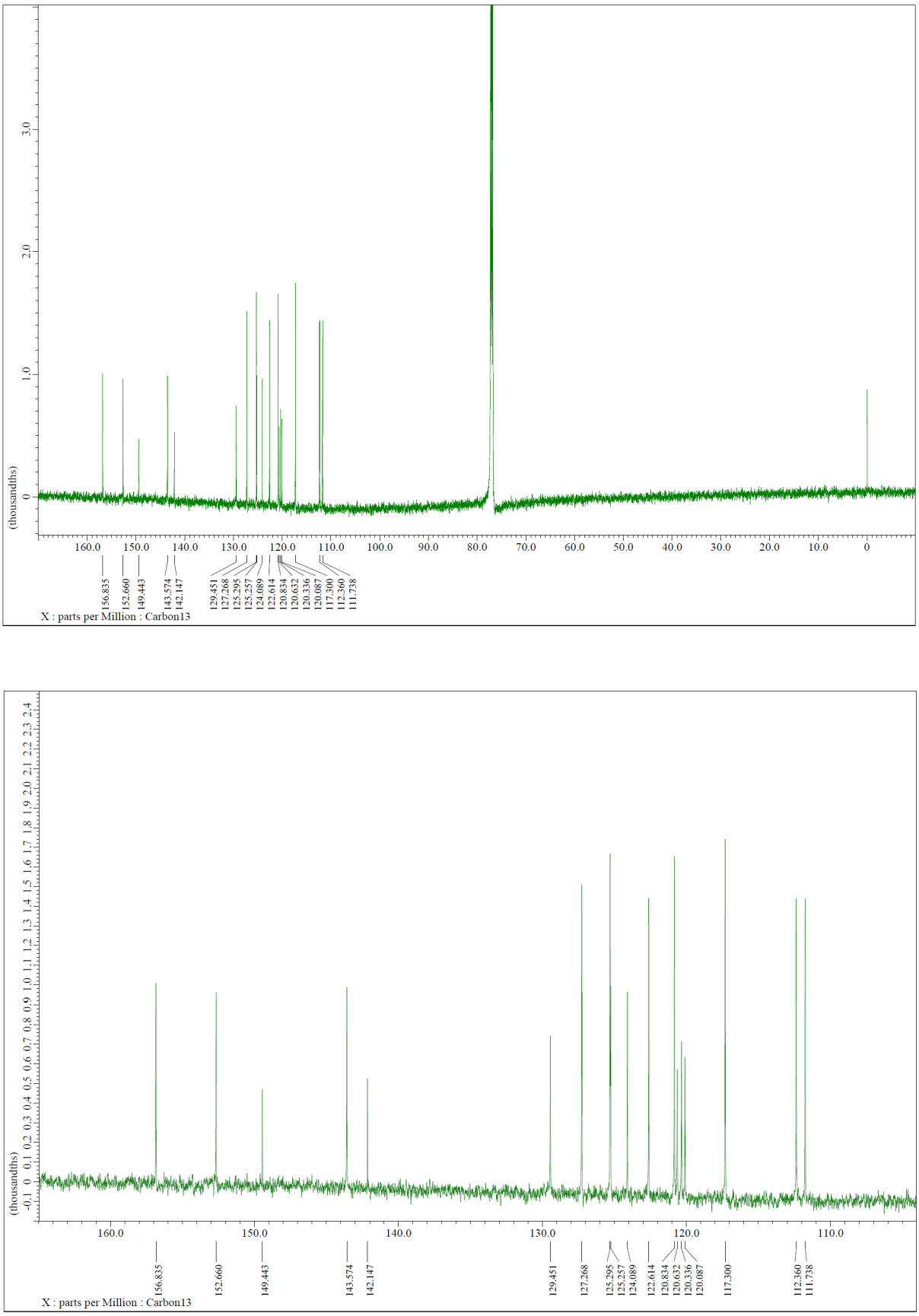

Figure S12. ^{13}C-NMR spectrum of **T2DBFBP** (151 MHz, $CDCl_3$, @R.T.)

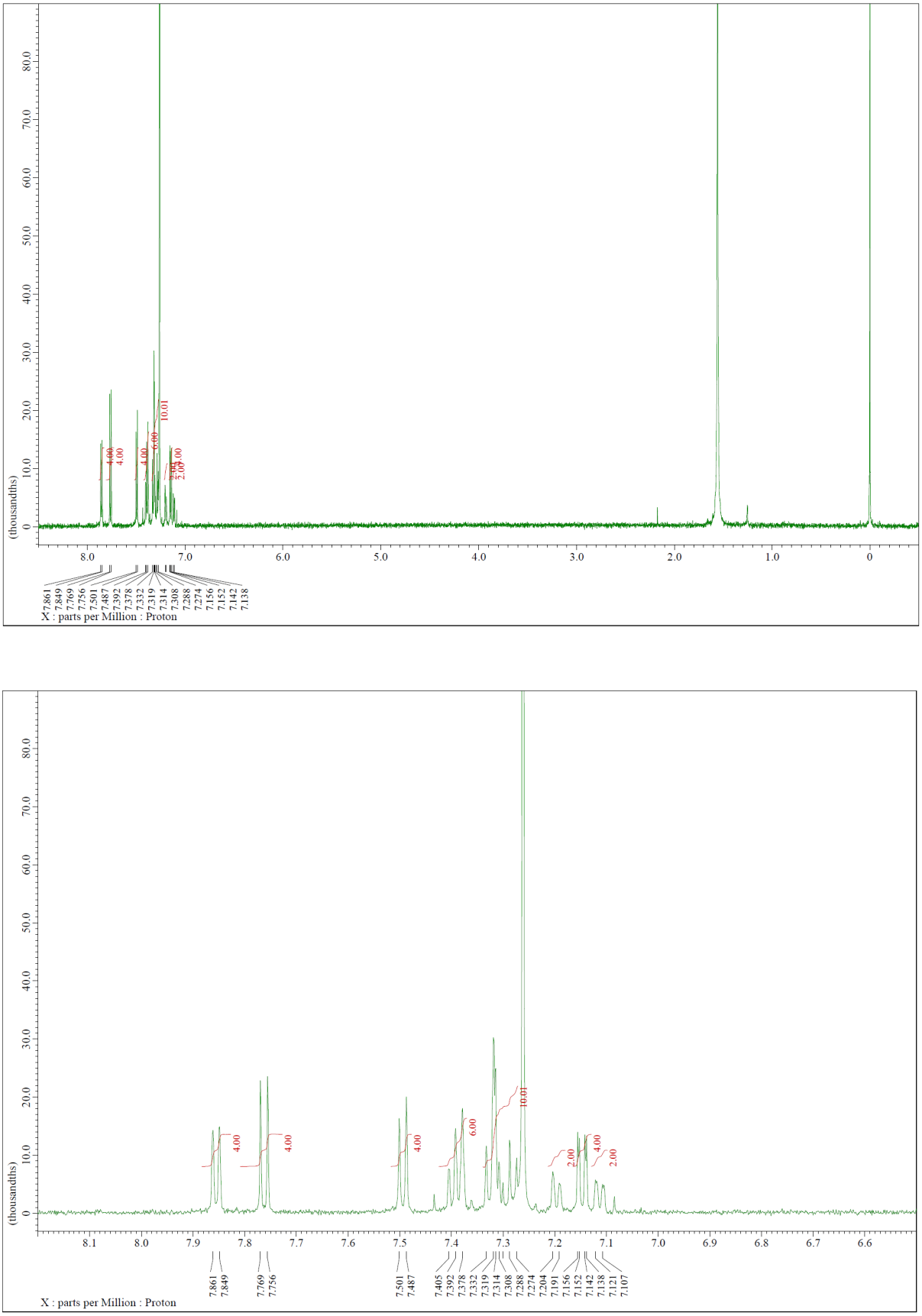

Figure S13. ^{1}H-NMR spectrum of **T3DBFBP** (600 MHz, $CDCl_3$, @R.T.)

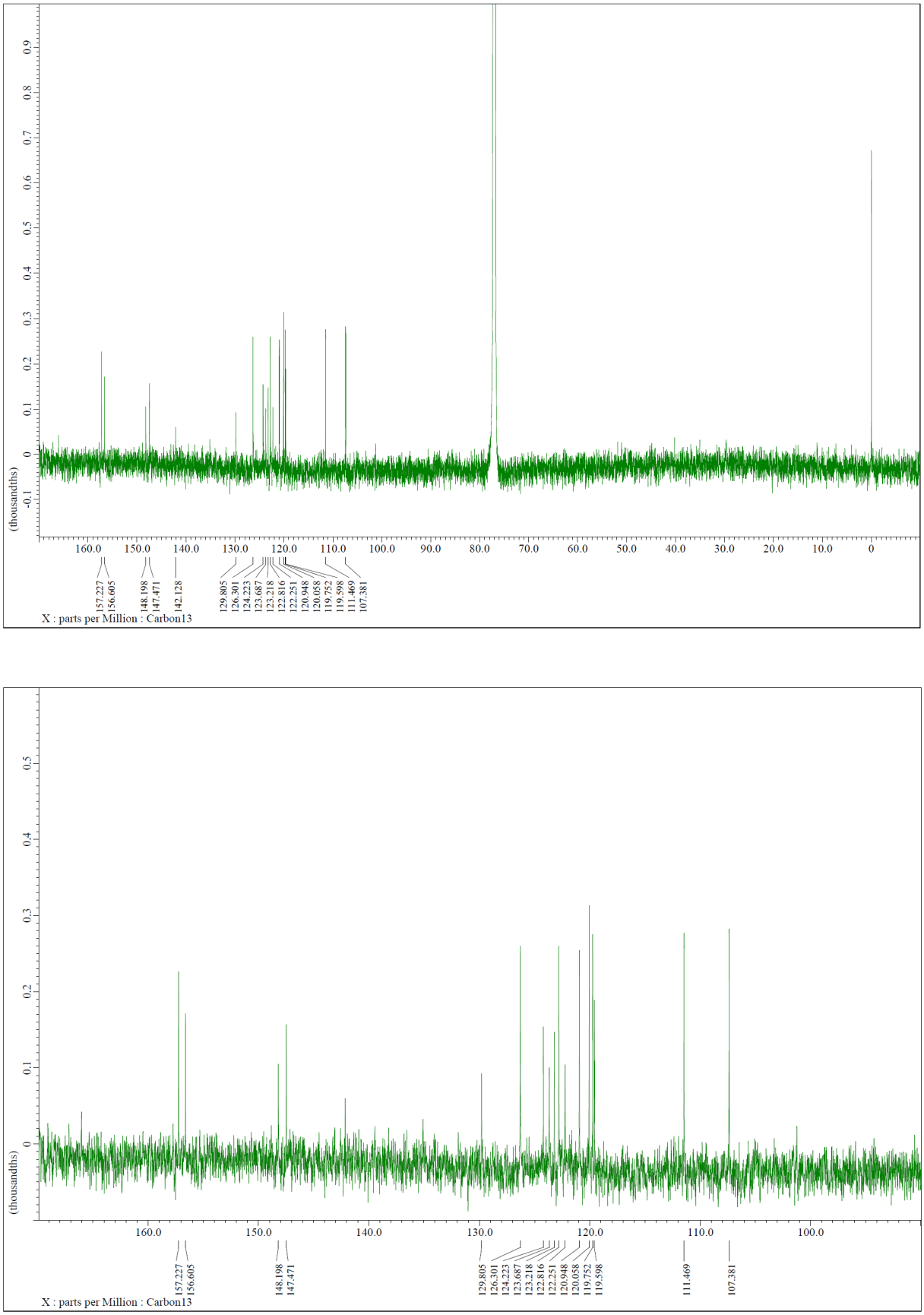

Figure S14. ^{13}C-NMR spectrum of **T3DBFBP** (151 MHz, $CDCl_3$, @R.T.)

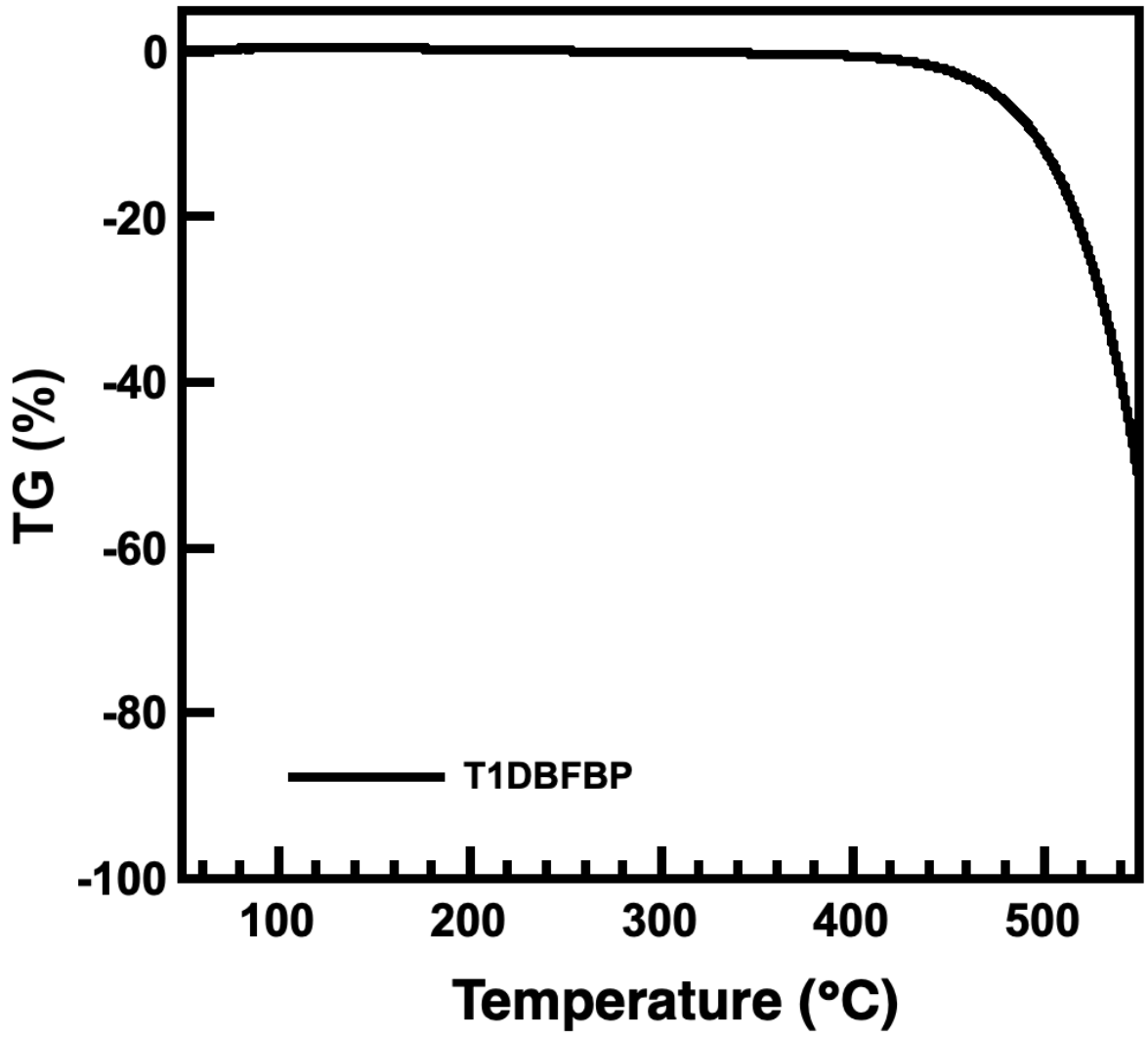

Figure S15. TGA thermogram of **T1DBFBP**.

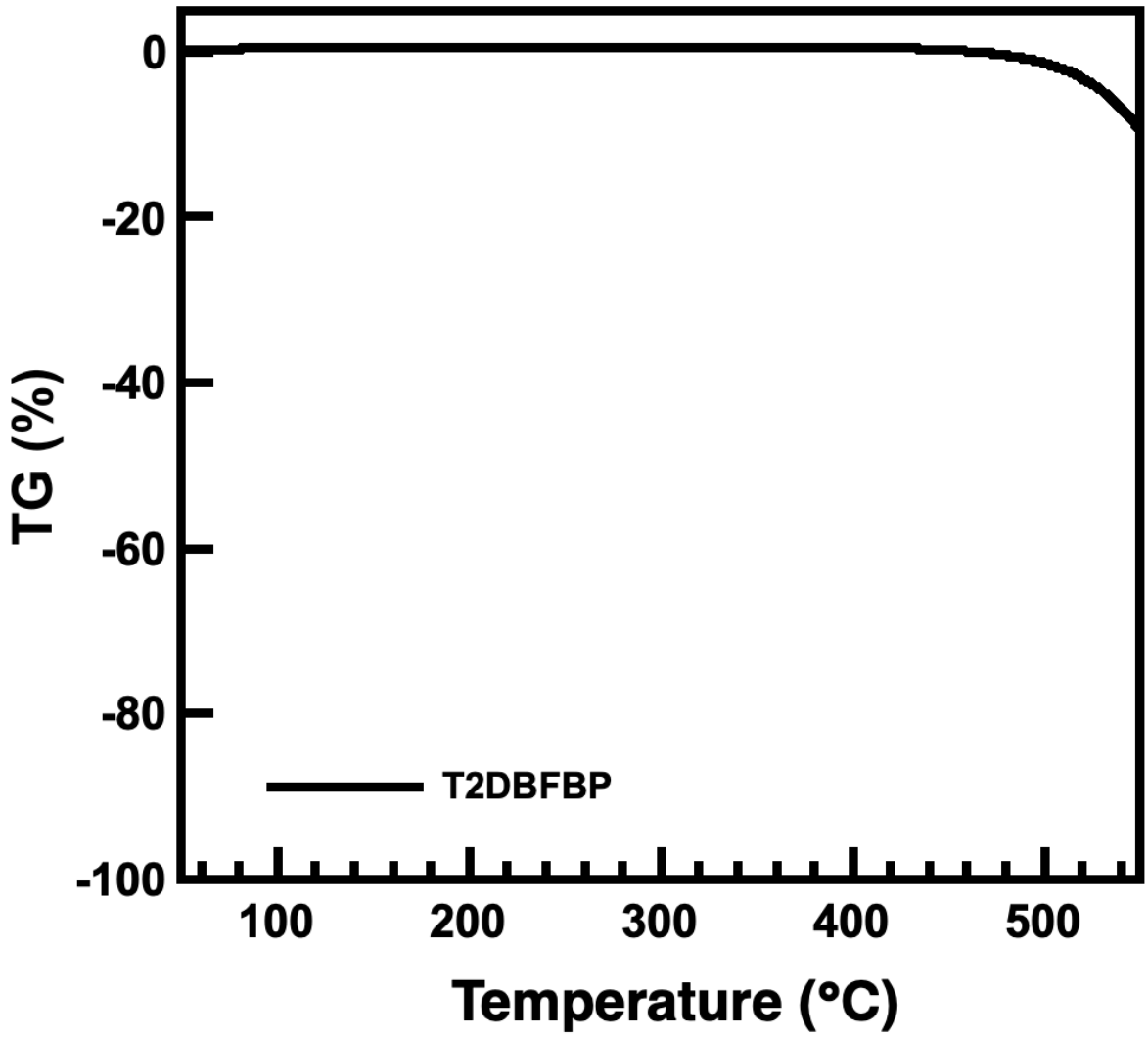

Figure S16. TGA thermogram of **T2DBFBP**.

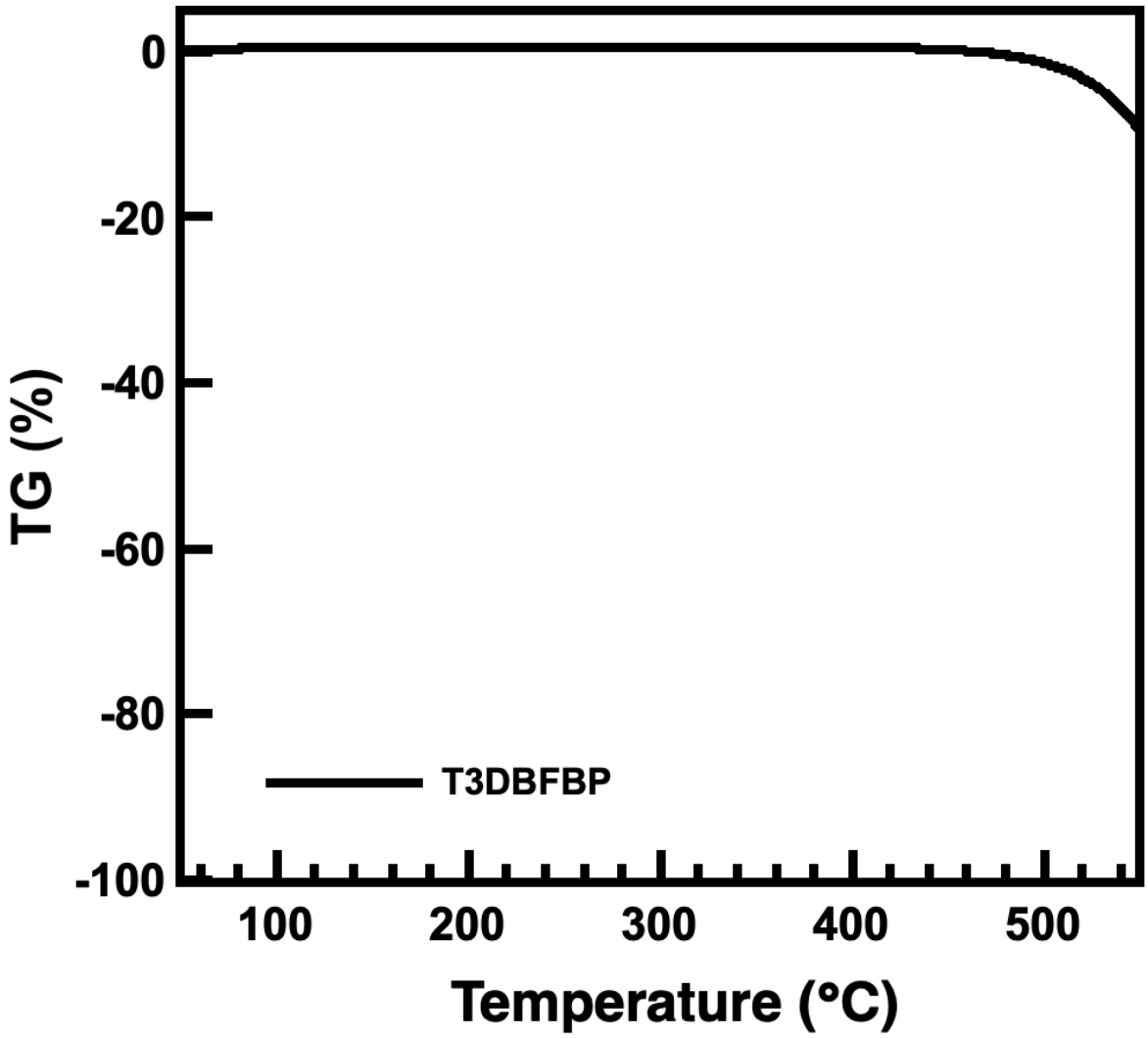

Figure S17. TGA thermogram of **T3DBFBP**.

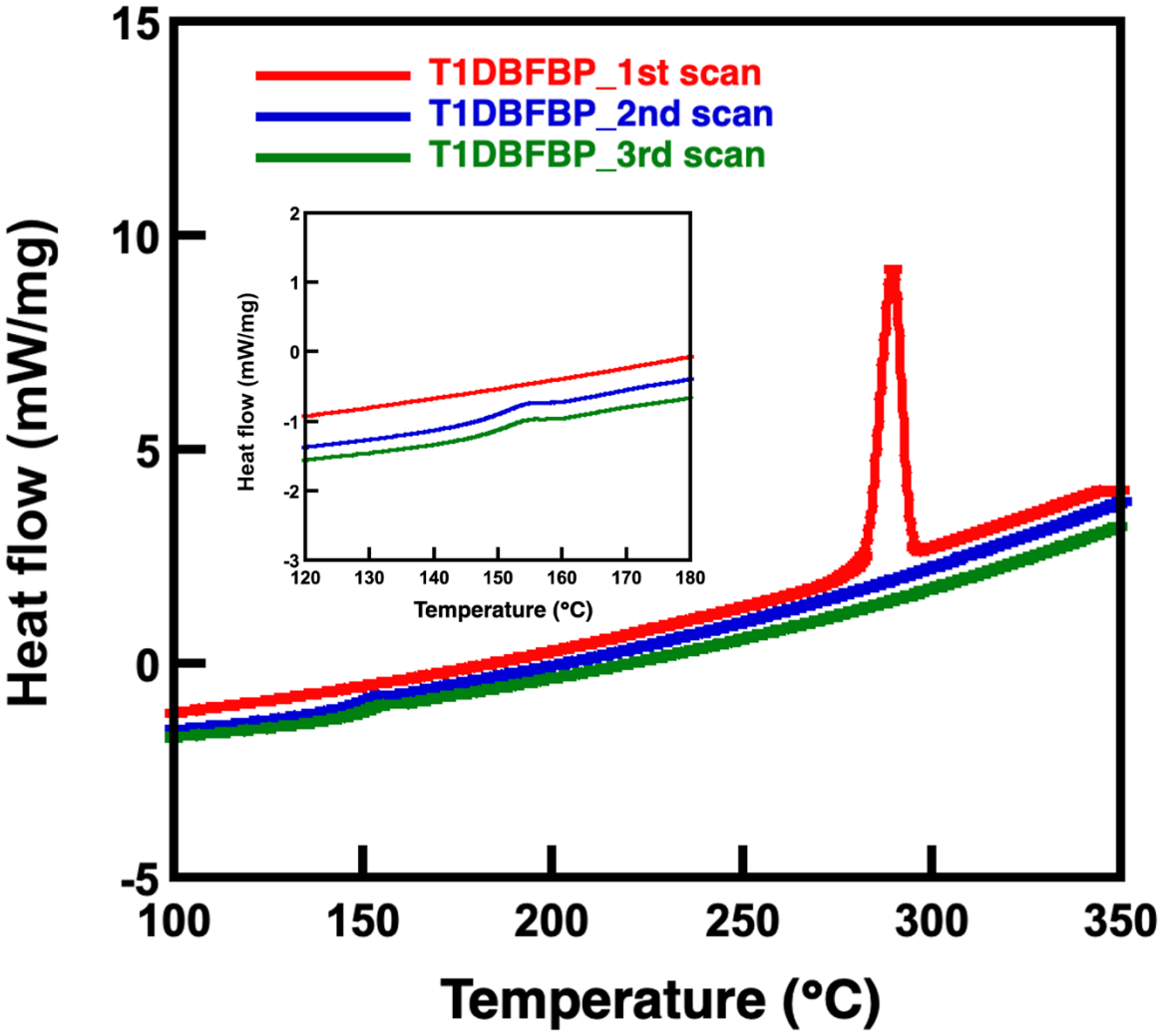

Figure S18. DSC curve of **T1DBFBP**.

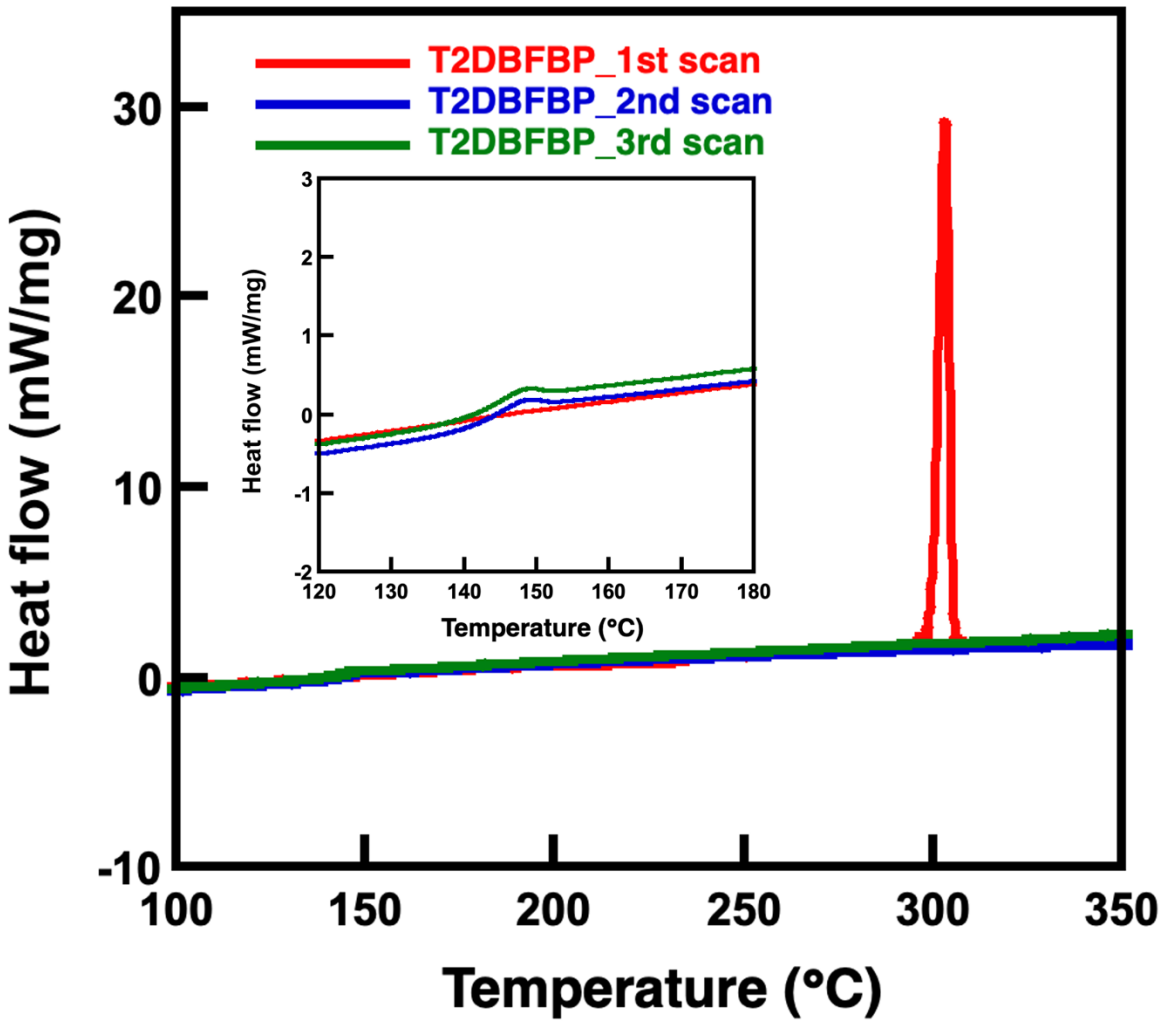

Figure S19. DSC curve of **T2DBFBP**.

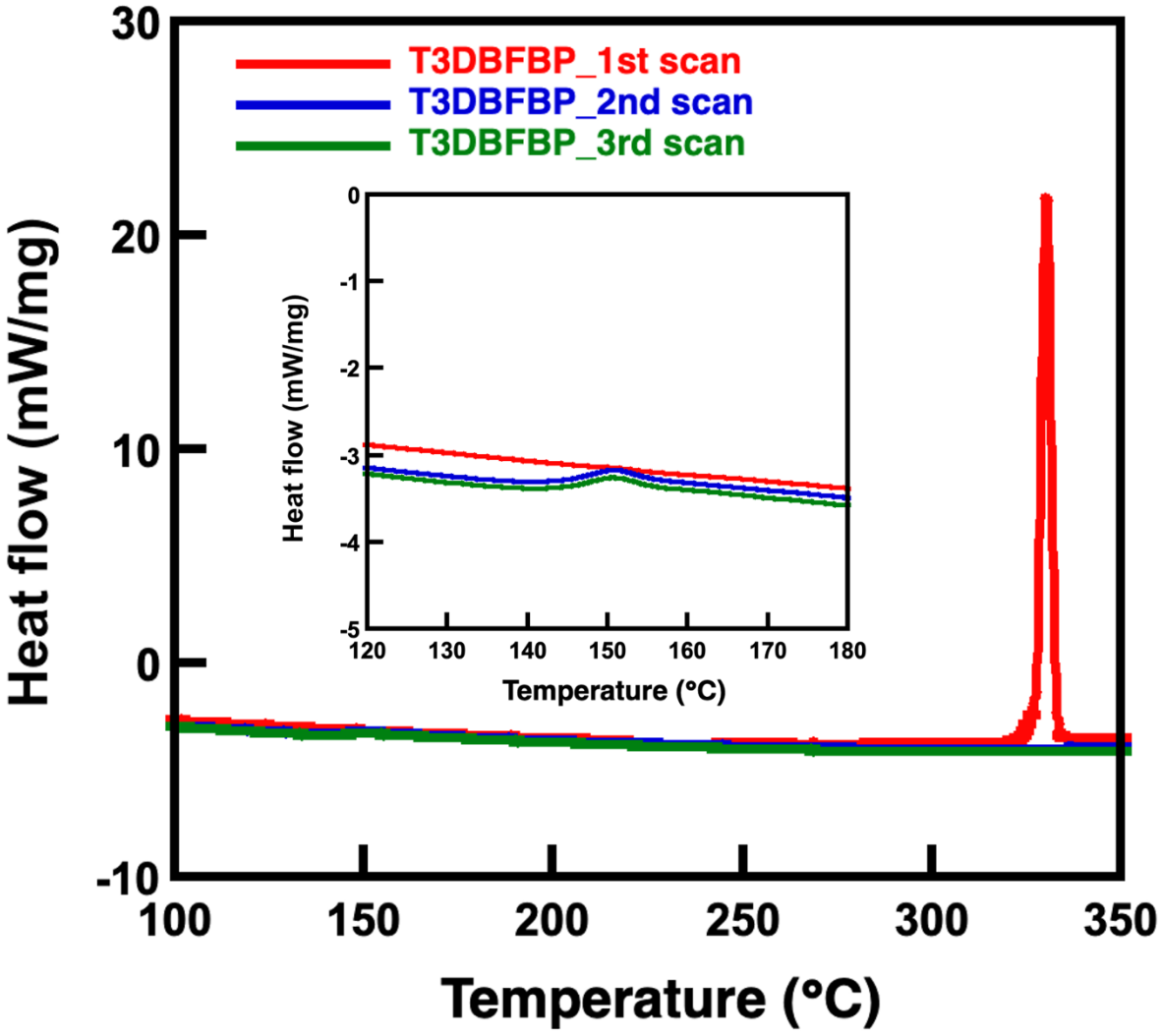

Figure S20. DSC curve of **T3DBFBP**.

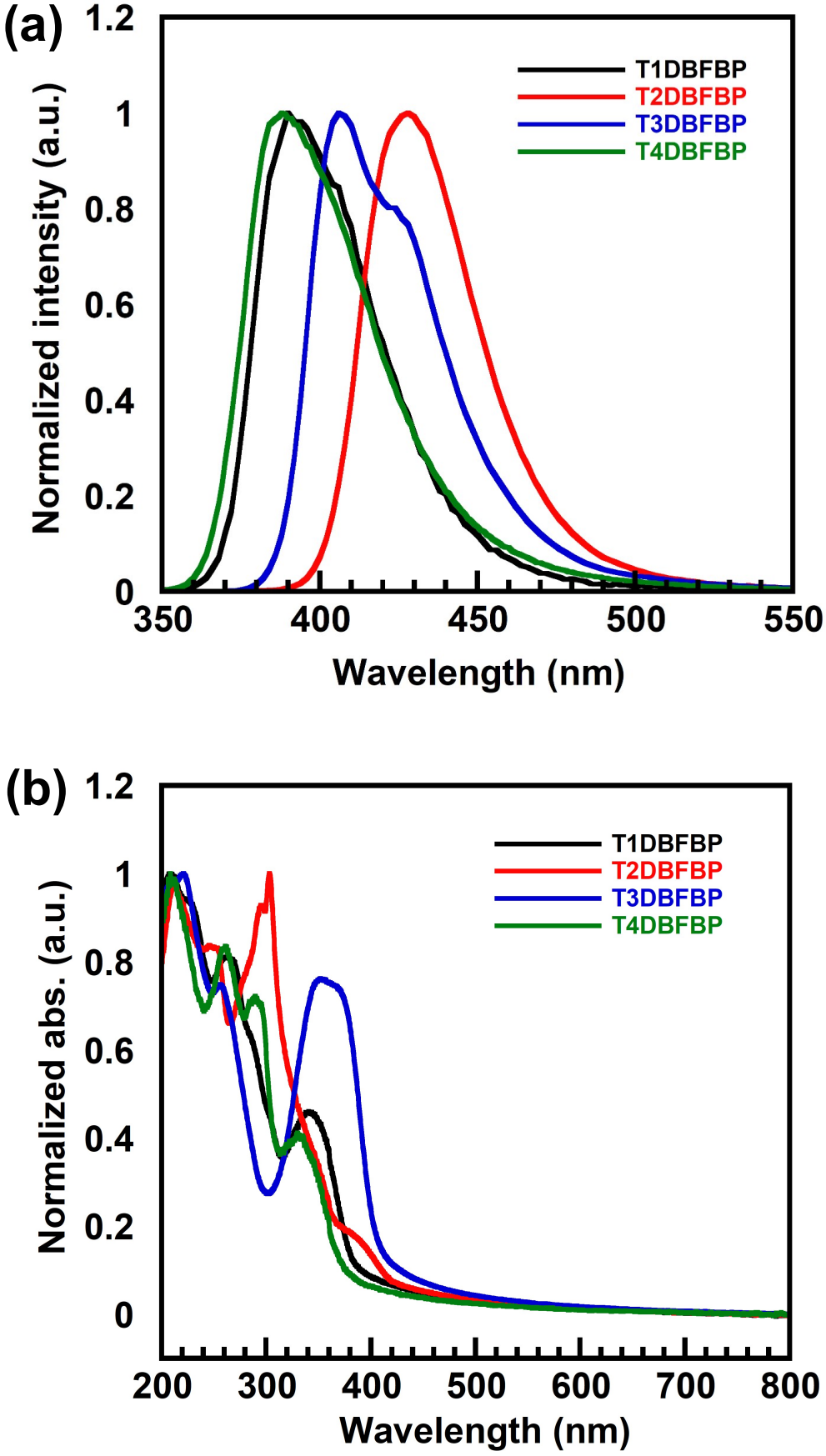

Figure S21. (a) PL spectra and (b) UV-vis absorption spectra of **TnDBFBP** films.

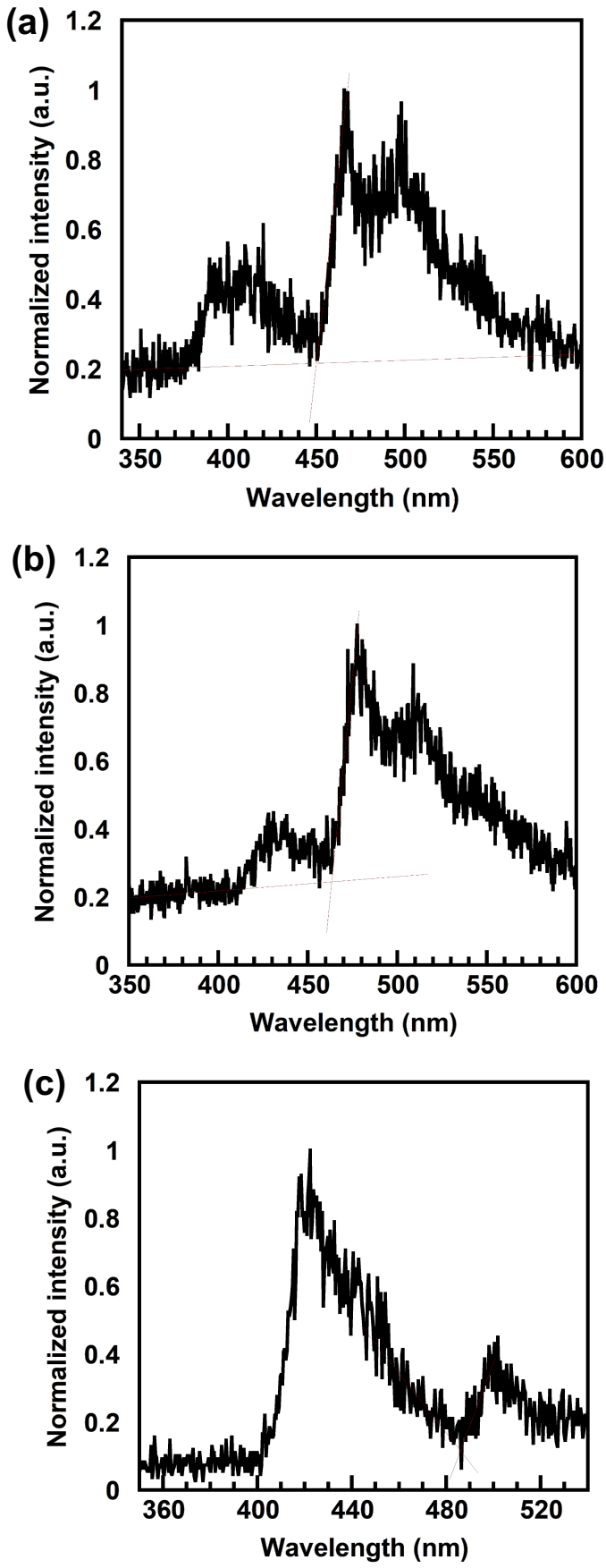

Figure S22. Phosphorescent spectra of (a) **T1DBFBP**, (b) **T2DBFBP**, and (c) **T3DBFBP** films at 5 K.

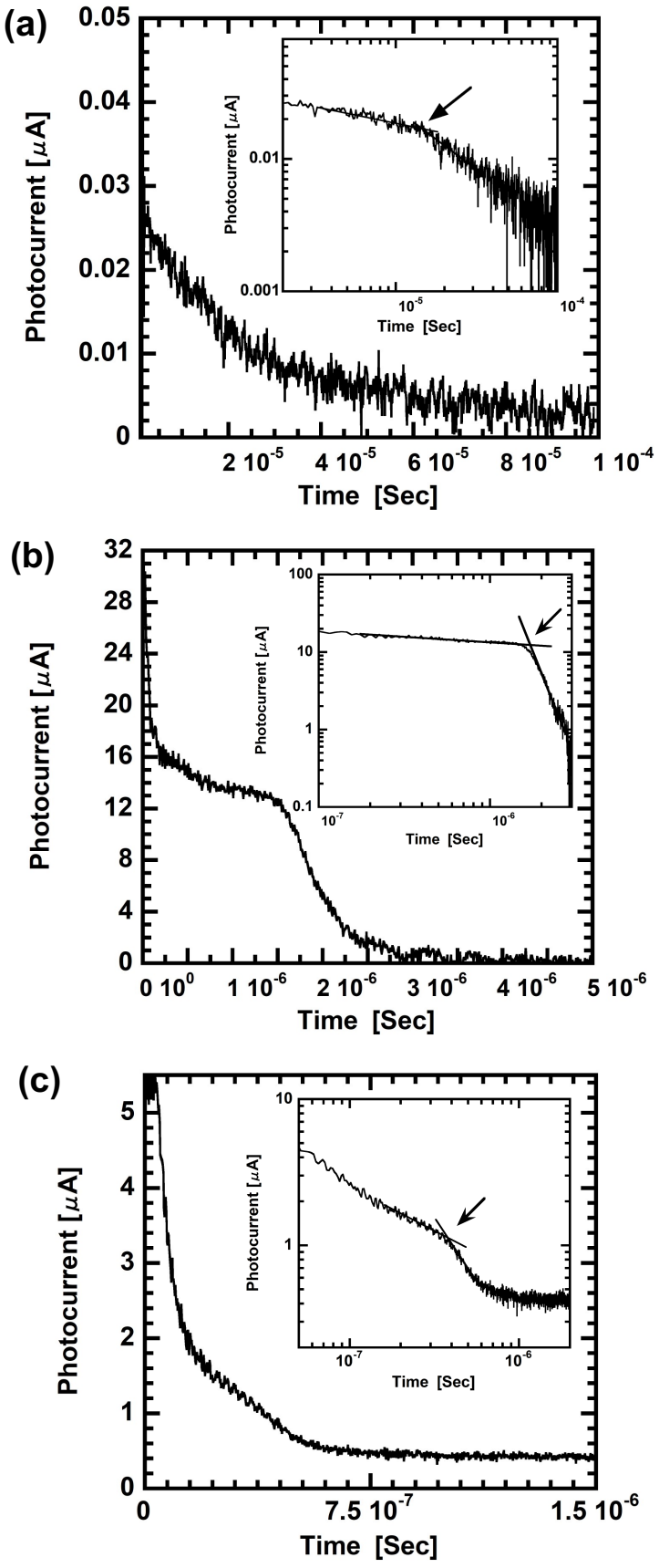

Figure S23. Representative TOF transients for holes at room temperature: a) **T1DBFBP** at E = 5.6 × 10^5 V cm^{-1}, b) **T2DBFBP** at E = 5.6 × 10^5 V cm^{-1}, c) **T3DBFBP** at E = 4.9 × 10^5 V cm^{-1}.

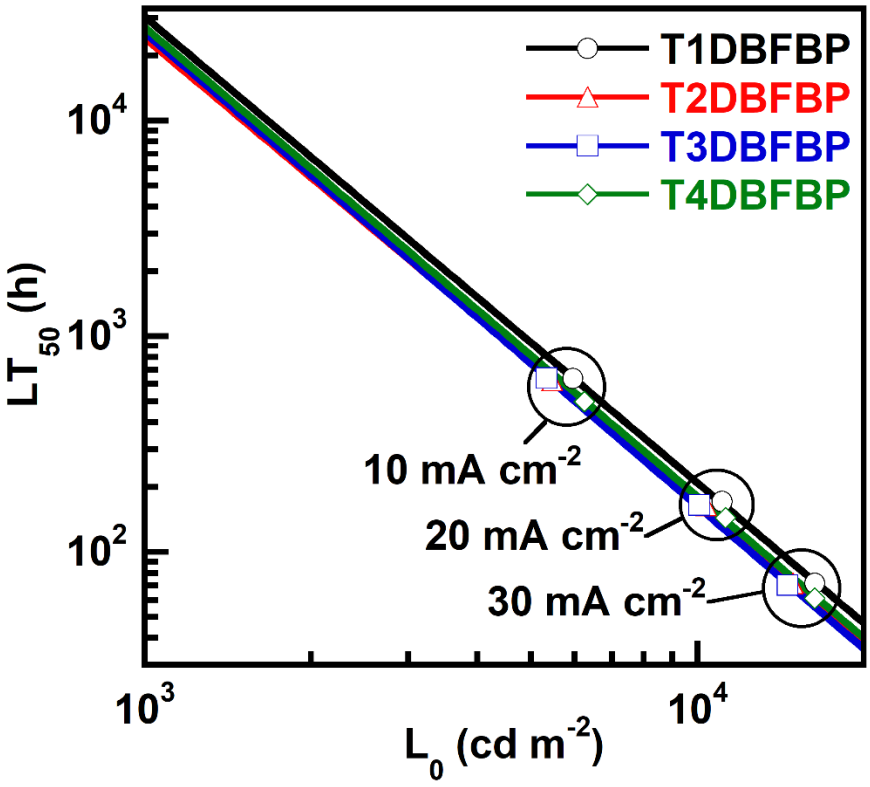

Figure S24. The results of the acceleration test at the constant current density of 10, 20 and 30 mA cm^{-2}.